Soft Mechanosensing via 3D Printing: A review

ADVANCED INTELLIGENT SYSTEMS
Open Access
www.advintellsyst.com

Soft Mechanosensing via 3D Printing: A review

*Diana Cafiso, Simone Lantean, Candido Fabrizio Pirri, and Lucia Beccai**

Recently, 3D printing, or additive manufacturing (AM), is emerging as a unique tool to fabricate soft mechanical sensors. Advanced performances can be obtained owing to the inherent 3D structures that enable enhanced and anisotropic deformations, to the multi-material approach, and to the seamless fabrication procedure leading to higher reliability. Nevertheless, despite the remarkable advantages, the printing of soft and conductive materials shows consistent challenges. This review provides an extensive analysis of the current progress of 3D printing of soft mechanical sensors, which mainly rely on resistive and capacitive transduction. First, the most common materials used are described, like soft matrixes, conductive fillers, and polymers. Then, the 3D printers that are most widely adopted for the fabrication of soft sensors are identified, and the specific advantages and the difficulties of each technology are examined. Finally, by reporting exemplary case studies from the literature, an overview of the scientific progresses on this topic is provided. The unique advantages led by 3D printing are highlighted, in terms of multiple materials, the feasibility of achieving complex geometries, and the advanced and programmed sensors properties.

1. Introduction

Soft robots are an emerging class of robots that, differently from their conventional and rigid counterparts, are able to perform precise and delicate tasks, e.g., they can comply with external surfaces through large deformation, squeeze and navigate in unknown and small spaces, recognize shapes and textures, grasp and move delicate objects, interact safely with humans.[1,2] They are made of "soft" materials, including any gel, colloid, foam, or polymer highly prone to deformation. The soft bodies of these innovative robots are inspired by living beings that can perform smooth actions and rapidly adapt to their surroundings.

In this regard, an efficient soft robot must include sensors that provide the perception of the environment and of the robot itself. Mechanical sensors are used to convert the deformations caused by mechanical stimuli into an electrical signal, which can be exploited for the robot control to grant effective and safe interactions between the soft robot and the surrounding. Due to the importance of sensing deformations, scientists researched various materials and technologies to develop soft mechanical sensors, i.e., mechanical sensors made of soft materials.[3–5]

Generally, soft sensors are fabricated via conventional manufacturing techniques such as casting,[6] tapering and pasting, and combining different parts (i.e., dielectric-conductive, substrate-electrode, etc.) in a step-by-step procedure. However, the so-produced devices suffer from poor adhesion due to the lack of mechanical and/or chemical compatibility between the various elements; moreover, the fabrication processes are excessively laborious, time-consuming, and with intrinsic low reproducibility and scalability. 3D printing, or additive manufacturing (AM), is a key technology to overcome these issues and move towards a new class of reliable and scalable soft sensors. It is one of the most disruptive technologies of the last decades that enables the fabrication of complex shapes by adding sub-units of material starting from a digital model,[7] in contrast to conventional, subtractive technologies. Due to the intrinsic design freedom and the possibility of using deformable materials, AM allows the implementation of complex soft robotic designs,[8] reaching applications in several fields such as biomedical engineering, healthcare, food, fashion, automotive, aerospace, etc.[9–14]

Besides the seamless fabrication procedure, AM guarantees the opportunity to build actual 3D geometries, unlike previous 2D and 2.5D fabrication technologies.[15,16] This aspect is crucial and opens technological possibilities such as: 1) inspiration from natural sensory receptors to guide new morphological designs, 2) enhancing the deformation of the bulk material by incorporating voids through lattice-like geometries, and 3) investigating designs that enhance deformations in specific directions. These new design principles can pave the way to develop soft mechanical sensors able to discriminate different types of mechanical stimuli (in terms of, e.g., direction of the externally applied force, frequency, spatial features, etc.) in a programmed way, leading to more reliable sensors for soft robots.

D. Cafiso, S. Lantean, L. Beccai
Soft Biorobotics Perception Lab
Istituto Italiano di Tecnologia (IIT)
Via Morego 30, 16163 Genova, Italy
E-mail: lucia.beccai@iit.it

D. Cafiso, C. F. Pirri
Department of Applied Science and Technology
Politecnico di Torino
Corso Duca degli Abruzzi, 24, 10124 Torino, Italy

The ORCID identification number(s) for the author(s) of this article can be found under https://doi.org/10.1002/aisy.202200373.

DOI: 10.1002/aisy.202200373

Nevertheless, whereby 3D printing represents a promising candidate, it shows several challenges that depend on the specific AM technology and the compromise between the material's processability and its mechanical and electrical properties. The current review tackles this aspect. The employment of AM to produce 3D-structured mechanical sensors is discussed by examining the material and technological aspects, with a particular focus on the typical mechanical transduction methods, i.e., resistive and capacitive. We identified the most common 3D printing technologies applied, reporting examples in the state of the art and discussing advantages and drawbacks to understand whether the AM represents an effective tool to construct 3D sensors for soft robotic applications.

2. Overview of Resistive and Capacitive Sensors

Mechanical sensors convert mechanical deformation into electrical response through various transduction mechanisms. Although there are numerous typologies of mechanical sensors, such as optical, inductive, piezoelectric, and triboelectric ones, the most common are those relying on capacitive and resistive transductions.[17] Their wide adoption is determined by the high performance, ease of fabrication, low cost, and simplicity of their read-out systems.[18] In particular, to the authors' knowledge, 3D-printed sensors reported in the literature are almost exclusively based on resistive and capacitive transduction. Herein, their working principles, main aspects, and limits will be briefly discussed, focusing on the relation between their sensing performance, deformation, and morphology.

In general, in these sensors, deformation induces a variation in the electrical resistance/capacitance measured by an external circuit.[19] As schematized in **Table 1**, the sensitivity (or the gauge factor) depends on the variation of such electrical signal. For capacitive sensors, this is caused mainly by a geometrical variation (i.e., the change in the distance between opposing electrodes); while, for the resistive ones, the crack propagation, the tunneling effect, and the disconnection in the conductive networks usually play a key role.[20]

Table 1. Working schemes for capacitive and resistive sensors. For the capacitive sensors, C is the capacitance, A is the area of the dielectric, d is the distance between the electrodes, ε_0 and ε_r are the vacuum dielectric constant and the relativity permittivity of the dielectric. For the resistive sensors, R is the resistance, ρ is the resistivity, l and A are the length and the area of the sensor.

	Capacitive Sensors	Resistive Sensors
	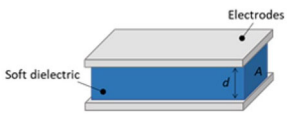	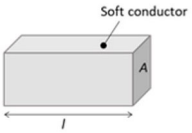
Transduction mechanism	$\Delta C = \varepsilon_0 \varepsilon_r \frac{\Delta A}{\Delta d}$	$\Delta R = \frac{\Delta \rho \Delta l}{\Delta A}$
Sensitivity	$\frac{\Delta C/C_0}{\Delta \sigma}$	$\frac{\Delta R/R_0}{\Delta \sigma}$
Gauge Factor (strain sensor)	$\frac{\Delta C/C_0}{\Delta \varepsilon}$	$\frac{\Delta R/R_0}{\Delta \varepsilon}$

However, all these factors are a consequence of the deformation following a specific mechanical stimulus; then, for both typologies, enhancing these deformations (i.e., creating softer sensors by means of materials and/or microstructures) is an efficient strategy to improve the sensitivity.

Furthermore, the performance of the sensors can be evaluated through other parameters, including the linearity of the electrical response,[17] the stability of the properties during the loading–unloading process (i.e., the lack of hysteresis), and the response time which, for polymer-based soft sensors, is delayed due to the viscoelasticity.[21] These parameters are fundamental to obtaining a durable and reliable sensor providing a predictable and efficient response.[22,23]

Usually, resistive sensors suffer from poor linearity and large hysteresis, in opposition to capacitive ones, which usually show a very linear behavior with negligible hysteresis and faster response.[22] The difference is ascribable to the diverse sensing mechanisms of the two sensors.[20] In contrast, resistive sensors usually offer higher sensitivity and ease of fabrication.[24]

3. Material's Aspects and Requirements

To fabricate soft sensors that fall in one of the transduction categories mentioned earlier, the processability and the properties of the materials involved must be considered. The materials must be classified as "soft" and conductive to provide a relevant electrical output signal once deformed. Moreover, they have to be easily processable and guarantee high electrical and mechanical performance and durability.

Stretchability and flexibility are the main requirements for the design of proper soft sensors. The term "Soft" refers to any gel, colloid, polymer, foam, and biological material highly prone to deformation. The typical characteristics are a low Young's modulus at room temperature or a shear modulus lower than 10 MPa[2] while maintaining a high strain limit. Among synthetic materials, this definition mainly encompasses polymers, especially elastomers and gels. Elastomers are amorphous polymers that undergo high deformation for low applied stresses and can recover their initial shape almost instantaneously once the load is removed. Otherwise, gels are biphasic materials consisting of a solid polymeric network and a liquid solvent, usually water (i.e., hydrogels).[25] The mechanical properties of these polymers can be tuned by different strategies. As an example, the mechanical properties of chemically cross-linkable elastomers can be adjusted by changing the amount of the crosslinker agents,[26] while the stiffness of hydrogels depends on the solvent's concentration. Furthermore, deformation recovery and fatigue resistance are crucial to limit the sensor's hysteresis (particularly problematic for piezoresistive sensors) and to improve durability in long-time applications.[22]

In addition to the intrinsic properties of the materials, also their geometry plays a crucial role in the final mechanical performance of the artifacts. For this reason, once again, 3D printing is promising, as designing complex shapes and voids may lead to unusual and programmable deformations within the material, which can eventually enhance the selectivity and performance of the sensor.[22] In this case, the properties are different from those of bulk material, and the stiffness must be properly

selected to fabricate the specific mechanical architecture of the sensor.

In addition to the mechanical requirements, the material must be electrically conductive to transduce an external stimulus into a reliable and measurable output. Although polymers are generally electrical insulators, intrinsically conductive polymers like polypyrrole, polyaniline, and *p*-poly(3,4-ethylenedioxythiophene) are now available.[27–29] Nevertheless, their low stretchability and conductivity ($<55\,000$ S m^{-1})[30] limit their use in soft sensing applications.

Therefore, another strategy to develop electrically conductive polymers is embedding conductive fillers within the polymeric matrix. Nevertheless, the addition of fillers often affects the mechanical performance of the material, stiffening the material and limiting its elongation at break. Therefore, a compromise between mechanical and electrical properties must be achieved. All of these aspects will be discussed in detail in the next section.

Finally, interlayer bonding must be considered when the sensor is composed of multi-material layers. A proper interface adhesion (chemical and mechanical compatibility) is needed to prevent failure when the sensor experiences large deformations and to ensure long-term applications.[31]

3.1. Soft Matrixes

The most common elastomers for the 3D printing of sensors are polysiloxanes (or silicones) and polyurethanes.

Silicones are 3D covalent networks composed of -Si(R)$_2$O repeating units, where *R* represents methyl, phenyl, vinyl, or trifluoropropyl group. Due to their rubber-like nature, their Young's modulus is generally low (maximum several MPa), and their elongation is above 300%.[32,33] Compared to the C—C bonds typical of organic compounds, the siloxane bond (Si—O) carries higher energy that endows the material with unique flexibility, heat resistance, chemical stability, electrical insulating, and ozone resistance.[33] Silicones are generally manufactured via injection and compression molding, or mold casting, and cured via a platinum-catalyzed hydrosilylation reaction that forms carbon-silicon bonds.[34,35]

Polyurethanes (PUs) are a family of polymers that are synthesized from the reaction between the hydroxyl groups (OH) of polyols and isocyanate functional groups (NCO), which result in the formation of urethane linkages. Their synthesis involves a diisocyanate, a chain extender that forms the hard segments, and a polyol that builds the soft segments. The Young's modulus and the other mechanical properties are determined by the microphase separation between these soft and hard segments, the chemical structure, and the preparation methods.[36,37] As a consequence, the Young's modulus ranges between 2 and 10 MPa, while the maximum elongation is generally around 400%.[37–40]

A wide range of PUs are available. Thermoplastics PUs are formed by low Tg segments that behave as the soft matrix, providing flexibility, and by segments with high Tg that reinforce the material by improving the mechanical strength as well as the chemical and thermal resistance.

Thermoset PUs derive from prepolymers cured by heat or a catalyst. They possess high mechanical and thermal resistance and superior hardness but suffer from poor durability.[36] Finally, PUs foams and fibers are widely employed for numerous applications, such as building engineering, thermal insulation, and electronics.[22,41–44]

A brief mention should be given to ionogels and conductive hydrogels. These materials are especially attractive for wearable electronics, as they are electrically conductive and optically transparent.[45,46] Diversely from hydrogels, the solvent of ionogels is an ionic liquid instead of water. Ionic liquids are organic salts with a melting temperature below 100 °C and an ionic conductivity from 10^{-4} to 8×10^{-2} S cm^{-1} which is, however, lower than those of conductive composite polymers.[47] Moreover, hydrogels are problematic for long-term utilization due to the dehydration of the solvent.[48,49] As a consequence, the applications of hydrogels and ionogels are still limited compared to those of elastomers.

All these materials possess mechanical properties (namely, Young's modulus and elongation at break) that define them as "soft". However, their mechanical behavior cannot be uniquely defined because it is determined by many factors, such as the curing mechanism and the polymeric backbone. For hydrogels and ionogels, the properties vary more significantly, as they are dictated by the solvent/solute ratio and by the polymer used. Nevertheless, it is possible to define a range of values for these materials from the literature, as reported in **Table 2**.

Furthermore, to print the soft materials in the three dimensions, it is necessary to fulfill other requirements, which depend on the specific technology discussed in the next sections of this review.

Nevertheless, shared issues are the adhesion between the printed layers and their self-standing ability. In fact, during 3D printing, each layer must withstand the weight of the following ones to build the object. In the case of soft materials, this can be hindered by their low mechanical strength, stiffness, and curing speed,[50] causing the deformation or the failure of the part during the printing process. Various solutions have been adopted to overcome the issue, such as the incorporation of additives (e.g., rheology modifiers) and polymers,[51] emulsions,[52] and the concurrent printing of supporting structures.[50]

3.2. Conductive Fillers

A wide variety of conductive fillers can be incorporated into soft polymers to fabricate deformable electrodes.

In general, the fabrication of composite materials leads to several issues, such as rheological modifications and variations in the processing temperatures and speeds, which may drastically affect the feasibility of the final product. According to the adopted

Table 2. Mechanical properties of most common matrixes for soft sensors.

Matrix	Young Modulus [MPa]	Elongation [%]	References
Silicones	0.2–0.7	>300	[32,127–129]
Polyurethanes	2–10	400	[36,37,39,40,130]
Hydrogels	Few kPa–10 MPa	400–3000	[131–135]
Ionogels	Few kPa–1.5 MPa	200–1000	[136–139]

3D printing method, different strategies are applied to overcome these challenges.

The concentration, distribution, and dispersion of the particles play a crucial role. Large aggregates act as defects and sources of cracks' propagation, embrittling and reducing the maximum elongation at rupture of the material. Aggregation is the result of various factors, such as the high concentration of fillers, the wettability factor, the strong filler–filler interactions, and the matrix–fillers compatibility. The latter has also a significant impact on the interface, which can be defined as the transition region where the matrix and the fillers are chemically or physically bounded.[53] The interfacial bonds represent a further crucial factor in composites' performance: a weak interface is detrimental to the mechanical strength of the composite and may lead to debonding at the interface, thus to the failure of the component. Therefore, it is necessary to find a good balance between the required electrical properties and the mechanical stability of the material.

The most common fillers applied in conductive polymeric composites can be categorized as carbon-based materials and metals. The formers encompass graphene, carbon black, and carbon nanotubes. In contrast, the most employed metals include gold, silver, and copper, which can be used in various shapes, such as plates, nanowires, and nanoparticles. Although metallic fillers offer higher conductivity (around 106 S cm^{-1}), they are prone to oxidation and are more expensive than carbonaceous ones.[26,54]

Regardless of the nature of the added particles, the fillers can impart electric conductivity into the composite material by arranging themselves in a continuous electrical pathway (i.e., the percolative network) through which the electrons can be transported. The minimum filler concentration that allows the formation of the percolative network, and therefore the transportation of electrons, is called the percolation threshold. This concentration depends on numerous factors, including the distribution, the size, and, precisely, the aspect ratio of the fillers. Higher aspect ratio fillers form the percolative network at lower concentrations because their geometry increases the probability of connectedness at low loads.[55,56]

Therefore, nanomaterials look very appealing for soft sensors, as they can impart conductivity at lower concentrations, preserving the mechanical behavior of the matrix in a cost-effective manner.[57,58]

4. 3D Printing Technologies for Soft Mechanical Sensors

Unlike conventional, subtractive manufacturing techniques, 3D printing operates by adding material in a layer-by-layer approach, starting from a digital file.

As shown in **Figure 1** the process starts with the computer-aided design (CAD) modeling of the object to be printed. Then, the CAD model is converted into a printable file (.stl), which defines the surface of the object into triangular meshes, and digitally sliced by a series of parallel planes with a constant interplane spacing that corresponds to the thickness of the layers. Afterward, the file can be sent to the apparatus and 3D-printed.

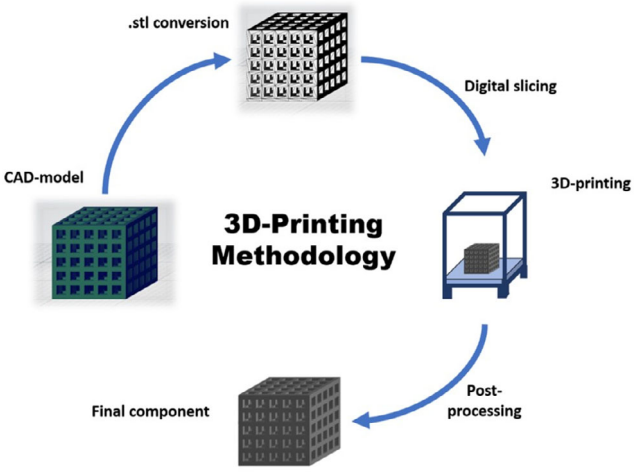

Figure 1. 3D printing methodology. The computer-aided design (CAD) model is converted into an .stl file and sliced in layers by the software. Then, the file is sent to the machine and 3D-printed. After the eventual post-processing steps, the final object is achieved.

Finally, various kinds of post-processing steps can be required depending on the technology to achieve the final object.[59]

The term additive manufacturing includes many technologies that can be classified as powder bed fusion, vat photopolymerization, material jetting, material extrusion, binder jetting, sheet lamination, and energy deposition techniques, according to the various printing principles.[60] In the soft sensing field, 3D printing has been adopted to fabricate one or more elements of the device (e.g., the dielectric layer of a capacitive sensor), the entire unit, or a mold for materials casting to tailor the geometry in an indirect approach.[61–63]

Overall, various 3D technologies were adopted in the literature, and the final soft mechanical sensors show an enhanced performance thanks to the specific 3D geometric features embedded. In this section are reported the most common approaches used for the manufacturing of 3D mechanical sensors, namely: fused filament fabrication (FFF); direct ink writing (DIW); and vat-photopolymerization (VP) technologies, which include stereolithography (SLA) and digital light processing (DLP, **Table 3**).

4.1. Fused Filament Fabrication

The FFF technology is based on the consecutive deposition of thermoplastic filaments that are molten together to form the final product. At the nozzle, the filament is heated above the melting temperature, Tm, so that it can be extruded through the nozzle on the building platform or on the previously printed layers; during printing, the filaments fuse together and solidify, after being cooled below their glass transition temperature Tg,[64] resulting in a 3D construct.[12,18] The quality of the final product (shape fidelity, aesthetic, surface finish, mechanical properties) is the outcome of different parameters associated with the machine, the working mode, and the material. There has been a continuous endeavor to optimize the combination of these variables, namely the layer thickness, the ratels' width and length, the build

Table 3. The most common 3D printing technologies for the fabrication of soft sensors, processable materials, and the fields of application.

	FFF	DIW	VP	
	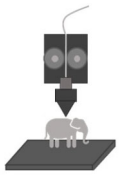	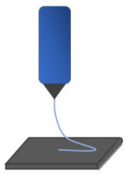	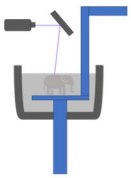	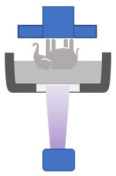
			Stereolitography	**Digital Light processing**
			SLA	DLP
Resolution	100 µm	1–100 µm	1 µm	20 µm
Polymeric materials	Thermoplastics filaments	■ High shear thinning polymers ■ Hydrogels ■ Silcones ■ Polyurethanes	• Low viscous polymers • Acrylate/Methacrylate elastomers • Photocurable (Hydro)gels	
Applications	• Rapid prototyping • Automotive • Molds for medical devices • Electronics	• Tissue engineering, • Bioprinting • Drug delivery • Electronics	• Microfluidics • Biomedical devices • Electronics	

orientation, the nozzle's diameter and speed, as well as the material's properties.

FFF printers allow easy implementation of the multi-material approach, which is of great interest for the fabrication of soft sensors, combining soft and compliance parts with conductive elements. However, FFF has intrinsic drawbacks such as lack of layers' adhesion, poor mechanical properties, and low surface quality, which is affected by the stair-stepping effect due to the nature of the process itself.[12,18]

Moreover, the most common polymers for FFF, such as polylactic acid (PLA), acrylonitrile butadiene styrene (ABS), polypropylene (PP), and polyethylene (PE),[65] do not belong to the class of soft materials. However, various compliant thermoplastic polyurethanes were developed by industries and are now commercially available.[32] Nevertheless, the processing of soft materials implies other issues mainly related to their low modulus. In particular, this can lead to buckling (due to the low ratio of the modulus to viscosity) and can affect the nozzles, e.g., causing slow refill or drooling.[66] Conductive polymers can be achieved by using fillers-decorated filaments rather than pure ones. Nevertheless, the FFF printing of composite filaments is limited by the restricted offer on the market since the in-house fabrication requires specific and expensive equipment and deep knowledge of the process.[67] Moreover, printing composites via FFF generally involves challenges, such as nozzle clogging, low surface finish, and the creation of internal micro-voids due to poor matrix/fillers interaction. Alternative solutions are represented by the in-nozzle impregnation approach and dual-head printing.[68]

The cost-effectiveness, ease of use, multi-material printing, and reliability of the process make FFF one of the most used printing technologies for fabricating soft sensors.

Li et al.[69] exploited FFF to develop a flexible resistive pressure sensor using thermoplastic polyurethane and graphene nanoplatelets composites. They modified the basic honeycomb shape by adding three and six supports for cell (**Figure 2**a–d) to create more complex structures. The finite element analysis (FEA) and the electrical tests demonstrate that, by changing the 3D structure, the sensor showed different deformability, thus diverse sensibility.

In particular, the presence of more supports led to an uneven distribution of stress and to a more pronounced stress concentration, which translates into a more enhanced deformation under compression. This resulted in higher sensitivity due to the rapid increase of the conductive paths caused by the reduction in the layers' distance under compression. As a consequence, the sensitivity of the sensors with more supports increased significantly at the same pressure. In particular, the gauge factor in the 0–3% deformation range varies from 13.7 (unsupported honeycombs) to 54.58 (honey-combs with six supports).

This work highlights the pivotal role of the 3D structure on piezoresistive sensors. In particular, the design freedom and rapid prototyping ensured by the 3D printing approach allowed the authors to investigate various shapes and geometrical parameters optimizing the sensing performances of the devices. It is important to mention that with conventional subtractive manufacturing techniques, these studies would be more time-consuming and some of the geometries would not be possible to be fabricated. Besides the geometry of resistive sensors, also the conductive material plays a crucial role. Davoodi et al. still investigated the role of 3D designs in the fabrication process and on the properties of piezoresistive sensors but with a different approach to developing the conductive material.[63] Instead of using composite filaments, they FFF-printed an ABS-sacrificial mold to develop a GNPs/Silicone compression sensor by dip coating to limit the impact of nanoparticles on the flexibility of the porous sensor (Figure 2e). In particular, the authors dip-coated the sacrificial mold in a GNP solution, then they pour the silicone, and finally dissolved the template to transfer the

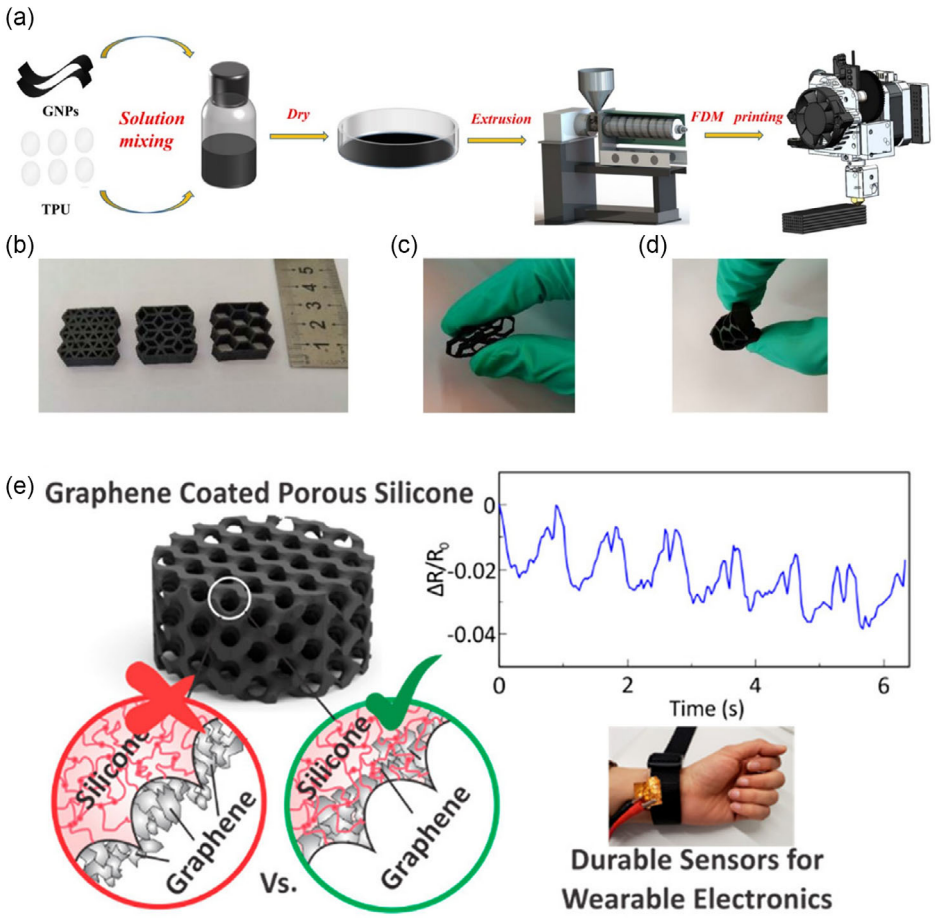

Figure 2. Sensors 3D-printed by means of fused filament fabrication (FFF) technologies. a–d) graphene/thermoplastic polyurethane (TPU) resistive sensor for strain and pressure. Adapted with permission.[69] Copyright 2021, IOP Publishing Ltd. e) Fabrication process of a GnP/silicone sensor through a sacrificial mold. Adapted with permission.[63] Copyright 2020, American Chemical Society.

nanoparticles from ABS to the sensor's surface. Dip coating the mold instead of the cured silicone led to a physical embedding of GNPs in the silicone matrix's surface, providing more stability to the sensor, even in harsh conditions (e.g., exposure to organic solvents). Moreover, the GNPs do not affect the deformability of the silicone rubber since the embedding involves only its surface.

The design of the 3D-printed sacrificial molds can be tuned to control the stiffness of the sensor of about one order of magnitude (from 70 to 660 kPa) with a consequent variation of the gauge factor ranging from 1 to 10. Besides the role of the geometry of the sensor, this work also proposes an interesting way to overcome the typical limitations of working with composite filaments in a FFF process. In particular, using the dip coating of a sacrificial mold, the authors were able to produce intricate and high-resolution geometries in a silicone-based material. This method is appealing to develop 3D sensors with materials that are not available as FFF filaments, enlarging the possibilities of AM technology application.

Yu et al.[70] printed a thermoplastic elastomer in a 3D shape to obtain a composite, piezoresistive sensor sensitive to both compression and strain. They used styrene-(ethylene–butylene)–styrene (SEBS) block copolymer to print the 3D samples, which were then immersed in the carbon nanotubes (CNTs) aqueous suspension and dried to remove the water (**Figure 3**). A further heating treatment allowed embedding the fillers in the SEBS molten surface, obtaining a higher CNTs/SEBS adhesion than that achievable by a simple coating process. As the conductive fillers are only embedded on the surface, the material still maintained high flexibility. By combining the intrinsic softness of the material and the complex 3D printed architectures, the piezoresistive sensors could be stretched up to 800%, and they showed a 6-fold larger gauge factor compared to the bulky material.

Furthermore, a 4 mm thick sensor showed a sensitivity of 136.8 kPa^{-1} at an applied pressure lower than 200 Pa. The researchers also focused on the thickness effect on the pressure sensitivity, assessing that the higher the thickness, the more the embedded CNTs can mutually approach, causing an increase in sensitivity. This aspect is not strictly related to the 3D structure, but it highlights the critical role of the geometric features in the sensors' performance. In this work, the authors implemented a highly stretchable 3D conductive material, overcoming one of the main challenges in 3D printing of soft sensors, i.e., developing conductive composites while preserving the flexibility of the

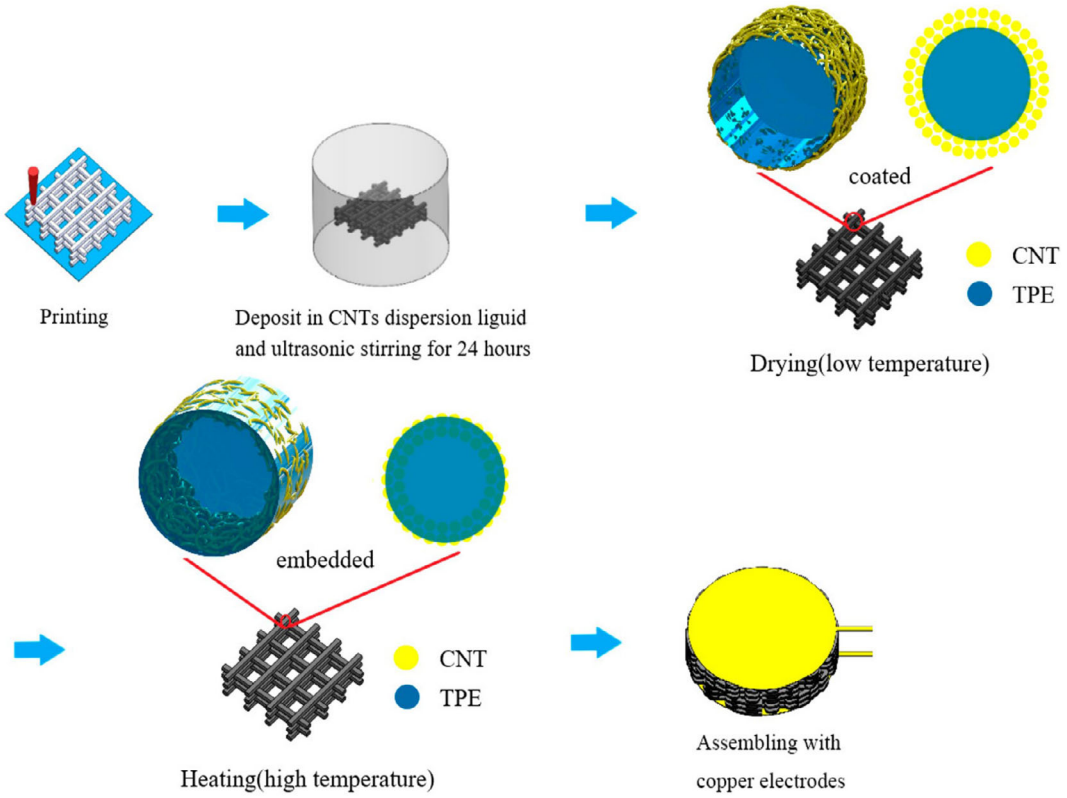

Figure 3. Carbon nanotubes (CNTs)/styrene-(ethylene–butylene)–styrene (SEBS) resistive sensor for strain sensing. Adapted with permission.[70] Copyright 2020, American Chemical Society.

matrix. Moreover, they obtained strain-sensing along one direction but for both compression and tension, due to the increasing and deconstruction of CNT paths, respectively.

4.2. Direct Ink Writing

Likely to FFF, DIW is an extrusion-based 3D-printing process. The material is stored in a syringe and extruded after applying pressure via a pneumatical compression or a screw.[71] To flow out from the nozzle, the material must possess proper rheological properties. First of all, it must show a shear-thinning behavior, i.e., its viscosity decreases under shear stress. Therefore, when the pressure is applied, the viscosity of the material is reduced, allowing the extrusion and the deposition of the layers. Furthermore, the flow of the ink occurs when the applied shear stress is higher than its yield stress (namely, the stress at which the material undergoes irreversible deformations); then, materials with low yield stress are desirable.[60] Once deposited, some inks demonstrate a good recoverability, which means that their viscosity increases again after stress release, forming a self-standing structure. When the material does not possess this feature, additional post-processing may be necessary to solidify the material, such as thermal curing, photopolymerization, or solvent evaporation,[64] which can be accomplished by adopting different printing heads.

Rheological adjusters can be added if the pristine material does not fulfill the rheological requirements. For instance, Suriboot et al. optimized commercial silicone (Sylgard 184)-based formulations to create printable inks for DIW.[72] They added dimethyldichlorosilane (DiMeDi)-treated silica fillers, which improve the thixotropic behavior of the materials as a result of the fillers' excluded volume and polymer–fillers interaction; the latest was enhanced by the incorporation of amphiphilic oligomeric additives (PEO-silane amphiphiles) of varying architecture. Durban et al. developed silicone inks with tunable stiffness (0.4–11.5 MPa), which consisted of vinyl terminated poly(dimethylsiloxane)-co-(diphenylsiloxane) (PDMS-co-PDPS) and hexamethyldisilazane-treated (HMDZ) silica.[73] The soft silicones were developed by incorporating hydride-terminated chain extension additives, which led to a Young's modulus of 0.40 MPa and an average elongation at a break of 528%. The inks were 3D-printed through DIW in structures with 250 μm of resolution. Equally to silicones, also PUs can be processed by DIW. Usually, the printing of these materials goes through their dispersion in solutions, with the synthesis of waterborne PUs overcoming the issues related to the use of organic solvents.[74,75]

In general, it can be stated that DIW offers the broadest selection of printable materials among the 3D-printing technologies, being suitable also for hydrogels,[76] ceramics,[77] epoxy resins,[78,79] photocurable resins,[80,81] and multi-material printing.[82]

As for the composites, the problems are the same as the other extrusion technologies: for instance, the unsuitable size of the fillers and agglomeration can cause nozzle clogging.

In the case of soft sensors, researchers can address the problem by embedding the conductive fillers after the printing process. Similar to FFF, DIW can be used to print soft samples that

are then coated with electrical material through dip coating. For example, Chen et al. 3D printed via DIW a cellular lattice silicon foam that was afterward covered with CNTs to obtain a resistive sensor.[51] The foam was produced through salt-leaching of an adequately designed ink containing PDMS and salt gels (NaCl microparticles, silicone oil, and dibutyl phthalate as solvent). After the printing and the thermal curing of PDMS, the salts and the liquid phase were removed by further steps, leaving microporosity in the 3D-structured foam, shown in **Figure 4**a. In particular, two porous networks were generated: the one caused by the salts removal and the other from the phase separation of immiscible DBP droplets. The foam demonstrated a hyperelastic behavior (maximum stretchability of 210%, near-zero plastic deformation after 10 cycles under 90% of compression strain). After being covered by CNTs, it could respond to compression stimulus (Figure 4b) and recover its electrical resistance after 10 cycles of 80% compression.

Nevertheless, DIW-printing of composite elastomers is achievable by accurately designing the material; moreover, the opportunity of multi-material can pave the way to a seamless fabrication of the device.[64]

As an example, Wang et al. embedded a hierarchically porous sensing element in a multi-modulus device (**Figure 5**) using an entire DIW process.[83] The authors combined a flexible elastomeric substrate and a pair of Ag/TPU double-helix electrodes with a microstructured NaCl/CB/TPU sensing unit (the NaCl was removed with water after printing). Moreover, they developed an ink with suitable rheological properties and three-level porosity, namely, the porosity between CB nanoparticles, the pores induced by the NaCl template, and the voids in the 3D architecture. The enhanced porosity granted high sensitivity across a wide pressure range and augmented the deformability under pressure. Contemporarily, the mismatch between the moduli of the sensor's elements and the electrodes' design minimized the resistance variation upon stretching and improved the signal-to-noise ratio. The sensor was assessed to be versatile for multiple applications, such as real-time monitoring of heart-pulse, the caption of weak human muscles' movements (e.g., blinking), and grasping ability.

These two works demonstrate the advantages of DIW compared to FFF in terms of material availability and customizability. Indeed, the authors were able to customize silicone-ink imparting high porosity. Moreover, Wang et al. were able to print the entire sensor in a seamless procedure, reducing the fabrication time and avoiding delamination issues at the interfaces between different components of the sensor. Their work proves that DIW holds the potential for fabricating sensors with enhanced performance and durability.

A mesoporous PDMS dielectric layer for a capacitive sensor (**Figure 6**a) was DIW-printed by Yang et al.[84] After printing and curing the PDMS, the authors fabricated the sensor by sandwiching the PDMS dielectric between two copper-plated polyimide films with a 3M tape. They demonstrated the impact of geometry on the rigidity and sensitivity of the devices. In particular, the DIW technology allowed the fabrication and investigation of different filaments stacking, thickness and spacing to determine the optimal microstructure design. The elasticity, regarded as a combination of PDMS and the air gaps, was higher

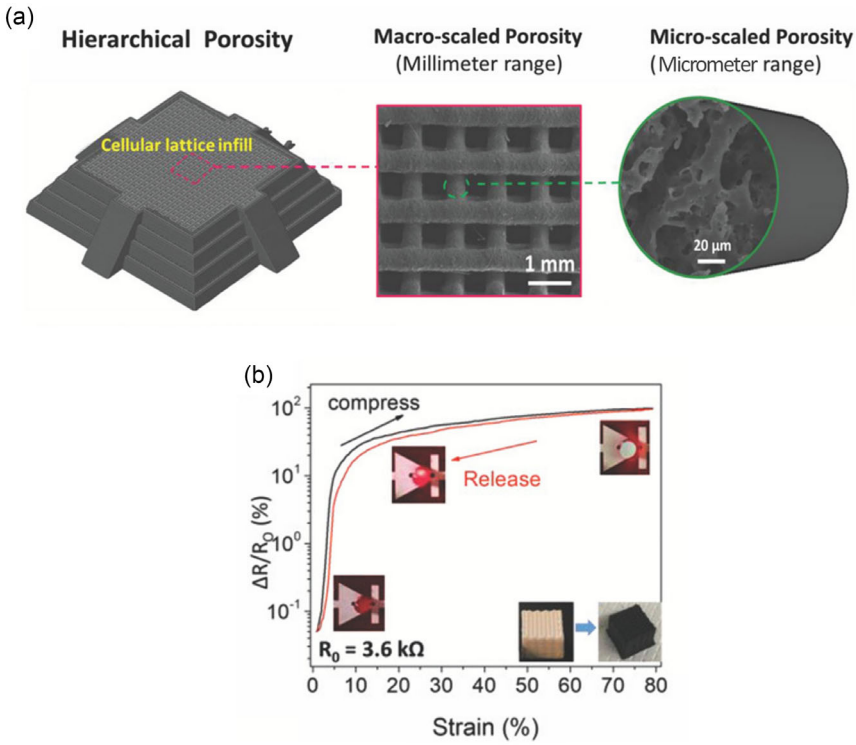

Figure 4. Direct ink writing (DIW)-printed resistive sensor. a) Hierarchical porosity developed in the poly(dimethylsiloxane) (PDMS) sensor. b) Resistive sensor achieved by covering the foam with CNTs. Adapted with permission.[51] Copyright 2019 WILEY-VCH Verlag GmbH & Co. KGaA, Weinheim.

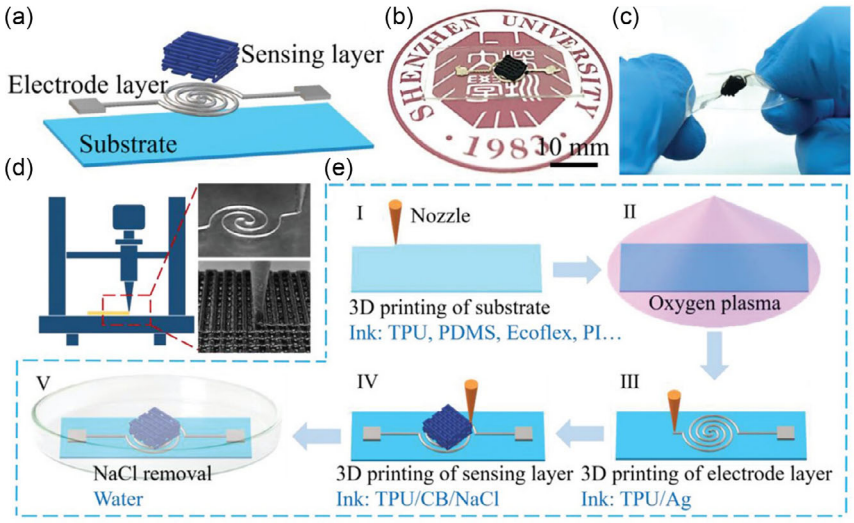

Figure 5. Full-3D printed multi-modulus sensor for pressure sensing. a–c) Multi-modulus and flexibile sensor with a 3D architecture. d–e) Fabrication process by DIW multi-material printing on a treated substrate, and by salts removal. Adapted with permission.[83] Copyright 2019, WILEY-VCH Verlag GmbH & Co. KGaA, Weinheim.

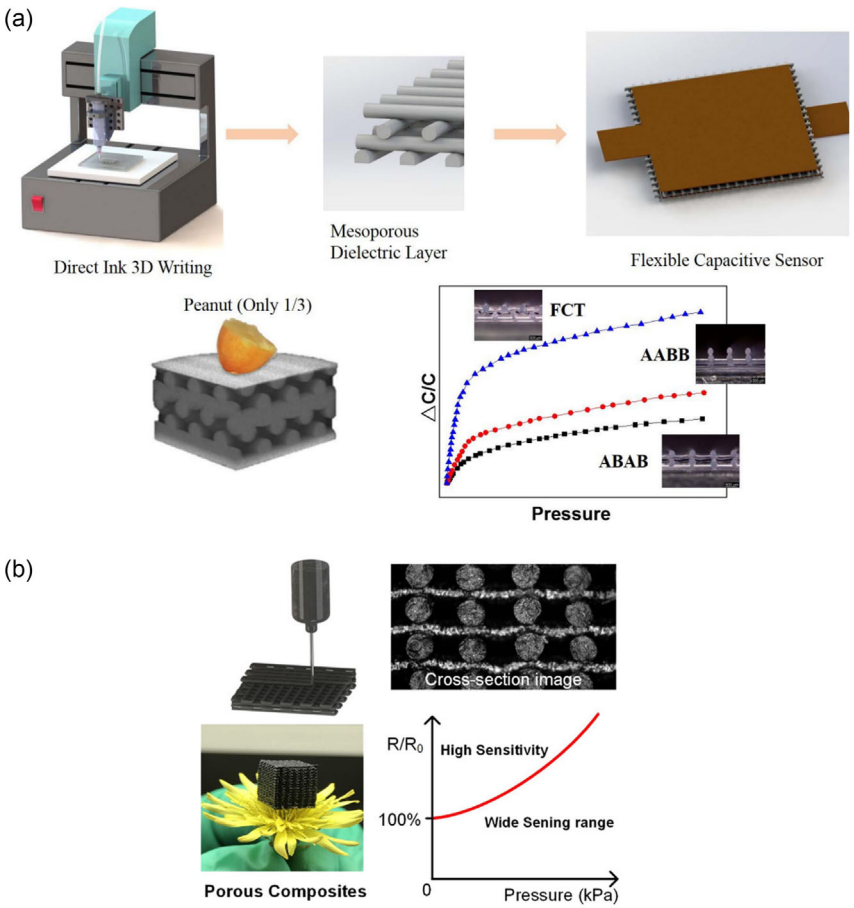

Figure 6. DIW-printed sensors. a) Capacitive sensor with a 3D-printed microstructured PDMS dielectric layer. Adapted with permission.[84] Copyright 2023, IEEE. b) CNTs/silicone compression sensor. Adapted with permission.[85] Copyright 2020, American Chemical Society.

for the structure with staggered filaments; for that device, the most proper fibers' thickness and spacing values led to a maximum sensitivity of 1.23 kPa^{-1} in the 0 to 0.4 kPa pressure range. Furthermore, the sensor was applied for haptic applications: the unit was integrated into a mechanical gripper to capture a plastic bottle by using the capacitance change of the sensor to measure the compressive force.

This work confirms that DIW can be exploited for fabricating 3D soft sensors with tailorable properties. With the assistance of FEA, the authors tuned the geometric parameters to emphasize the deformation under a given stimulus, thus the sensitivity. Nevertheless, the sensor was manufactured step-by-step by tapering different materials. Despite practicality, this approach may limit the opportunities of DIW printing due to the weak bonding at the interfaces between the different materials. This aspect suggests that multi-material printing for sensors still needs to be optimized, and new contributions are expected from the scientific community.

Furthermore, as Tang et al. demonstrate, design strategies can be combined with material aspects to achieve unusual properties.[85] They used DIW to print a flexible sensor with a tunable (positive or negative) piezoresistive effect, as shown in Figure 6b. CNTs were added to a silicone precursor (Ecoflex 0020) to develop a conductive ink. Moreover, several CNT-fumed SiO_2 nanoparticles (SiNPs) weight ratios were investigated to tune the rheology and produce a DIW printable formulation.

Furthermore, the top and bottom electrode layers were fabricated separately in a flexible silicone paste that maintained the adhesion with the sensing unit under deformation. Compression tests showed that the printed specimens had a modulus ranging between 60 and 150 kPa. This enabled high deformation and enhanced sensitivity. Under compression, the sensor was subjected to different states of deformation (reduction or expansion) according to the position of the microstructure's elements causing more changes in the charges' migration path due to the 3D shape. In particular, sensors with lower CNTs loading led to a positive piezoresistive effect, i.e., electrical resistance increased with increasing pressure.

The authors DIW-printed a soft mechanical sensor with complex architecture and a tailorable piezoresistive effect. They developed sensors with positive piezoresistivity showing a low Joule effect and an excellent trade-off between high sensitivity (0.096 kPa^{-1}) and working range, which is required from many human-robot applications (e.g., health monitoring and tactile sensing).[85] Therefore, this result is promising for printing endurable sensors with different behaviors that can adapt to several real applications and requirements.

4.3. VP: Digital Light Processing and Stereolithography

The vat-polymerization (VP) technologies rely on irradiating a tray containing a liquid formulation, which polymerizes in a 3D object through a chemical reaction, namely a photopolymerization. Hereafter, the photopolymerization process will be overviewed briefly for the readers' convenience. A photocurable system contains an organic molecule, the photoinitiator, able to absorb light and generate reactive species (typically radicals or cations) that can initiate the chain polymerization of the monomers (i.e., the building blocks of a polymer) via the radical or cationic mechanism.[86] Radical photopolymerization is the most extensively used for VP-3D printing as it allows faster kinetics.[87,88] Typically, the photocurable formulations are composed of the photoinitiator, monomers, oligomers, and other additives, such as dyes and fillers, to improve the resolution, the processability, and the properties of the final polymer.

The VP techniques are stereolithography (SLA) and digital light processing (DLP), which differ because of the irradiation modality. The DLP apparatus consists of a dynamic mask formed by micromirrors that irradiate each layer simultaneously, whereas SLA cures each layer point-by-point through a movable laser beam.[89] The DLP irradiation method ensures higher fabrication speed, but the resolution is generally lower than SLA's. However, the recent developments of the last years improved the resolution that both technologies can achieve (1 μm for micro-SLA and 10 μm for DLP), limiting the mismatch.[90,91]

Among the different parameters, the light intensity, the time of irradiation, and the formulation composition play a key role in the final resolution and properties of the printed part. Generally, the optimization of those parameters is the result of a trial-and-error process.

Regarding the processable materials, the palette of available photocurable polymers is low and typically limited to thermoset acrylates and methacrylates, as they present fast reaction kinetics. These are generally stiff and fragile, so the fabrication of soft objects by VP-3D printing is already a challenging task. The formulation must contain fast reactive monomers to be successfully 3D-printed. Moreover, the viscosity must be tailored as high viscosity may affect and hinder the printability of the resin.[92] A common strategy to widen the range of printable soft materials is to acrylate (i.e., to functionalize the polymer chains with ending acrylic units) different monomers. Acrylate polyurethanes and silicones can be developed to produce soft prepolymers that polymerize under light irradiation.[15,93,94] For instance, acrylate-PDMS has been 3D printed via DLP printing,[95,96] as shown in **Figure 7**. In the case of polyurethanes, this challenge can be addressed by synthesizing the material from fatty acids or blending it with low-molecular-weight polymers.[97,98]

In contrast, the processing of silicones involves further challenges. The material's choice is restrained to silicone oligomers because low viscosity is required; furthermore, silicones are highly permeable to oxygen, making them sensitive to oxygen inhibition. This effect, namely the interaction between oxygen and radicals during the photopolymerization, hinders the chains' growth and the polymerization process,[32] affecting the printability by VP technologies.

Concerning this latter aspect, a valid alternative is represented by the so-called thiol-ene photopolymerization, based on the radical catalyzed addition of a thiol to a vinyl functional group, which can be adopted to improve the oxygen resistance, as well as the reaction rates.[99] This reaction mechanism led to the successful VP-printing of silicones by means of both DLP and SLA.[100–102]

In the context of this review, it must be highlighted how the addition of conductive fillers enhances the struggles in the VP-3D printing of soft matrixes. Besides increasing the viscosity of the formulation, fillers may compete with the photoinitiator in the light's absorption,[103] affecting the photoreaction and resulting in slow kinetics or failed polymerization.

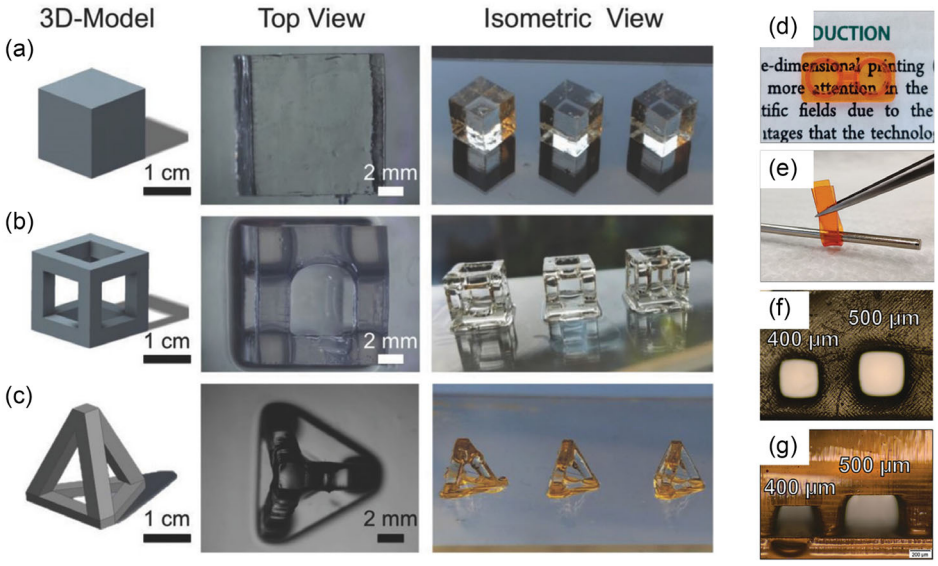

Figure 7. 3D-printed PDMS by: a–c) Bhattacharjee et al. (adapted with permission[96]) Copyright 2018, WILEY-VCH Verlag GmbH & Co. KGaA, Weinheim and d–g) Gonzalez et al. (adapted with permission[95]) Copyright 2020, WILEY-VCH Verlag GmbH & Co. KGaA, Weinheim.

Despite these issues, the VP-3D printing technologies ensure the finest resolution and accuracy among the various AM methods; thus they became appealing in the manufacturing of intricate-shaped sensors.

As shown in **Figure 8**a–e, X.Yin et al. 3D-printed via DLP a capacitive sensor employing a dual-material printing approach.[104] The sensor was fabricated by alternatively printing two photocurable precursors: a conductive hydrogel (compound of polyamide,

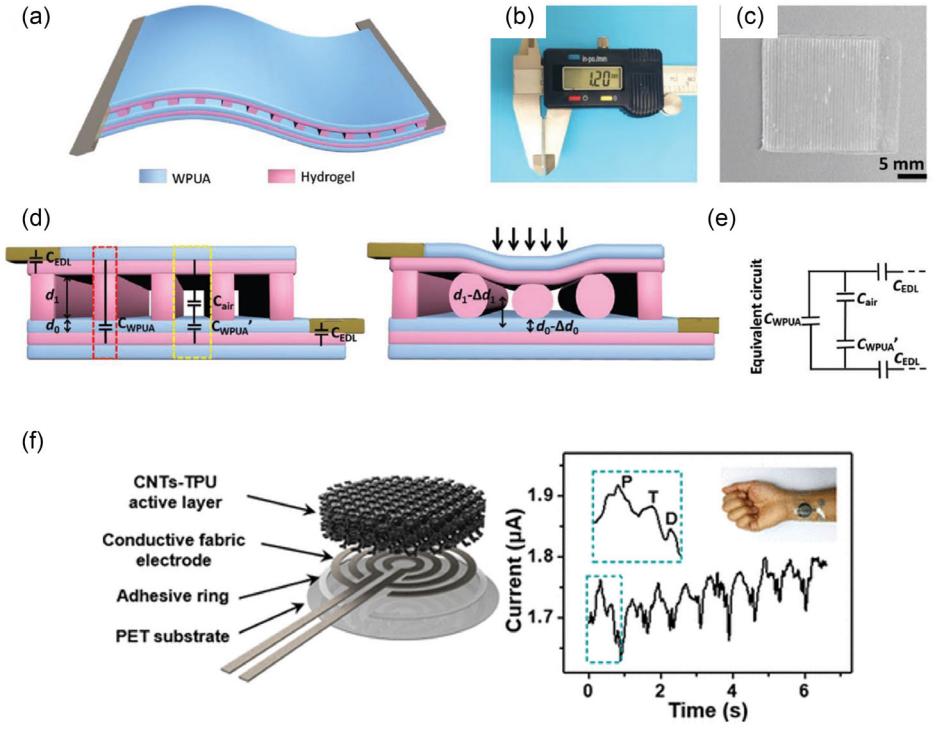

Figure 8. a–e) A full-printed capacitive sensor fabricated via DLP, composed of acrylate water-soluble polyurethane and an acrylate hydrogel. Adapted with permission.[104] Copyright 2019 WILEY-VCH Verlag GmbH & Co. KGaA, Weinheim. f) CNTs/TPU pressure sensor. The acrylate TPU was printed via DLP and then coated with the conductive fillers. Adapted with permission.[106] Copyright 2021, American Chemical Society.

polyethylene glycol diacrylate, and Mg^{2+} ions) for the electrodes and a water-soluble PU as the soft dielectric. To achieve multi-material printing, the researchers used two resin tanks, replacing one with the other after a given number of layers. By doing so, they exploited the two acrylate resins' similar polarities and chemical structures to form a strong chemical bonding between the electrodes and the dielectric. The excellent interface limited the dehydration of the hydrogel ensuring good performance stability.

One of the electrodes was structured in beams to give larger deformability. The researchers observed that taller beams and wider beam spacing resulted in more sensitivity, ranging from 0.4–0.6 kPa^{-1} below 1 KPa of pressure and from 0.25 to 0.37 kPa^{-1} in the range 1–5 KPa. However, excessive air gaps (i.e., high, spaced beams) caused the fluctuation of the electrical signal. Then, the structure's geometry was selected to achieve a compromise between sensitivity and stability. As a result, the all-printed sensor presents good sensitivity to pressure and excellent durability over 10 000 loading–unloading cycles within the pressure range of 0–1 kPa.

The authors used DLP to build an all-printed sensor with complex geometries. The high resolution of DLP enhanced the freedom of the design, which was exploited to adjust the geometrical parameters and optimize the sensor's performance. Notably, the multi-vat approach reduced the fabrication time; it also limited the issue of the dehydration of the hydrogel, representing an encouraging result for the development of durable hydrogel-based ionic skins.

Multi-material approach was similarly used by Mu et al.[105] They fabricated a hollow capacitive strain sensor by DLP-printing a commercial acrylic resin and multi-walled carbon nanotubes (MWCNTs). Increasing fillers' concentration led to increasing conductivity and viscosity, affecting the processability of the ink through DLP. Therefore, the optimal amount of MWCNTs was selected as a compromise between electrical performance and viscosity; the printing parameters were also settled regarding the optical change caused by the opaque fillers. By a multi-vats approach, the scientists could print dielectric (acrylic resin) and electrodes (acrylic resin/MWCNTs) in a full 3D process. The dielectric and the top electrode were shaped in a hollow configuration to enable larger deformation. The sensor demonstrated capacitance change with pressure and good repeatability under cyclic loading.

This work, similarly to the previous one, highlights DLP's potential for multi-material printing. Even if the choice of the materials for this 3D printer is limited to photocurable resins, the presence of similar chemical groups in these polymers can be easily exploited to form strong chemical bonding between the different inks. Therefore, DLP can be used to fabricate sensors rapidly and in a reproducible manner while improving their durability and performances.

Another proof of successful DLP-3D printing of a soft sensor was provided by Yin et al.[106] The authors printed a lattice CNTs/ acrylate thermoplastic polyurethane (TPU) sensing layer for a pressure, capacitive sensor (Figure 8f). First, DLP was exploited to fabricate the green TPU model, which, afterward, was coated with a thin layer of CNTs through an ultrasonic probe treatment. The acrylate TPU lattice could be DLP-printed in a plethora of sizes, proving its feasibility in producing both high-resolution, tiny structures and larger components in a relatively short time. The pressure sensing mechanism relied on the contact between the sensing 3D unit and the electrode, more the contact between the rods of the deformed lattice microstructure. In particular, five representative lattice models were investigated, and the most sensitive structures were those that experienced larger deformation under the same load. Therefore, the optimal combination of the lattice's design and layer thickness produced the highest sensitivity of 1.02 kPa^{-1}, a pressure detection range of 0.7 Pa–160 kPa, and a stable electrical response for 60 000 cycles under 10 kPa.

This work demonstrates that DLP printing is a feasible approach to easily scale sensors in size and geometry, thus expanding their range of applications. Moreover, the researchers developed a conductive coating on the printed sample. This approach avoids the concerns related to the DLP printing of composite resins allowing the fabrication of structures with finer resolution.

Similarly, Peng et al. printed polyurethanes through DLP to create a robust and flexible strain sensor (**Figure 9**) that was coated with a conductive hydrogel.[107] The authors used three kinds of polyols to synthesize three types of polyurethanes acrylate oligomers, demonstrating that the one containing the poly(tetrahydrofuran) units (PPTMGA) offered an optimal combination of mechanical strength and elasticity. In fact, its soft segments, composed of routable C—O and C—C groups, provided the highest elongation at break (≈400%), while the hydrogen bonds in the hard segments endowed the resin with good tensile strength (15.7 MPa) and fatigue resistance (100 compression cycles at 80% strain). The researchers adjusted the viscosity through the addition of reactive diluents and printed complex structures with a resolution of 150 μm. To fabricate a sensor, the DLP-printed lattice component was soaked in a UV-curable pre-hydrogel aqueous solution containing also lithium chloride. Then, the hydrogel/lattice component was irradiated to cure the hydrogel and create bonds between the unreacted acrylates on the elastomer's surface and the hydrogel's monomers. This caused a robust interface between the two materials of the sensor, which exhibited a sensitivity of 2010 MPa^{-1} (under compression of 0.09–0.23 MPa), owing to the hollow structure that ensured large deformation.

In this work, the authors used a salt-filled hydrogel to produce a conductive coating. Using a hydrogel instead of nanomaterials (e.g., graphene, CNTs) may be appealing to avoid long-term fatigue due to the breakage of the interface between the rigid fillers and the soft matrix.[108] Moreover, the chemical compatibility between the hydrogel and the elastomeric matrix enabled the fabrication of a stronger bonding. This approach is valuable for fabricating endurable soft sensors, even if using hydrogels still poses the issue of the water's evaporation. Nevertheless, the possibility of adopting different materials to impart conductivity is appealing to exploit the high resolution of VP-printers to construct sensors with complex architectures and advanced properties.

An example of an SLA 3D-printed soft sensor is offered by Cai et al., who developed a transparent and conductive elastomer based on a mixture of maleic acid (MA)/choline chloride (ChCl) and acrylamide (AAm)/choline chloride type polymerizable deep eutectic solvents (PDESs).[109] The sensor, shown in **Figure 10**, appeared highly transparent and could be shaped in intricate geometry. Moreover, the abundance of –COOH,

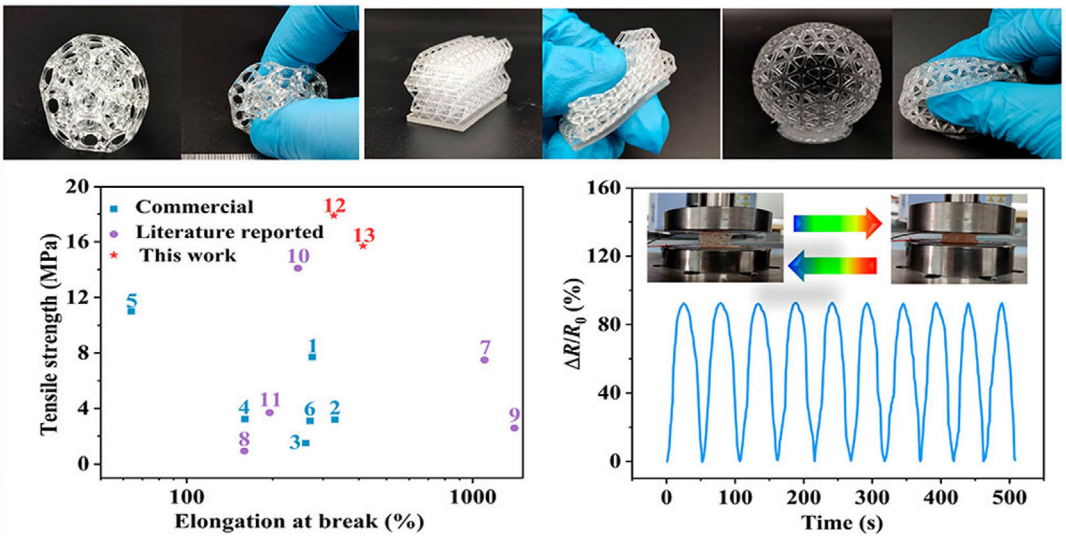

Figure 9. 3D printing of a 3D object that was immersed in an ionic hydrogel precursor and cured via UV to obtain a compression sensor. Adapted with permission.[107] Copyright 2020, American Chemical Society.

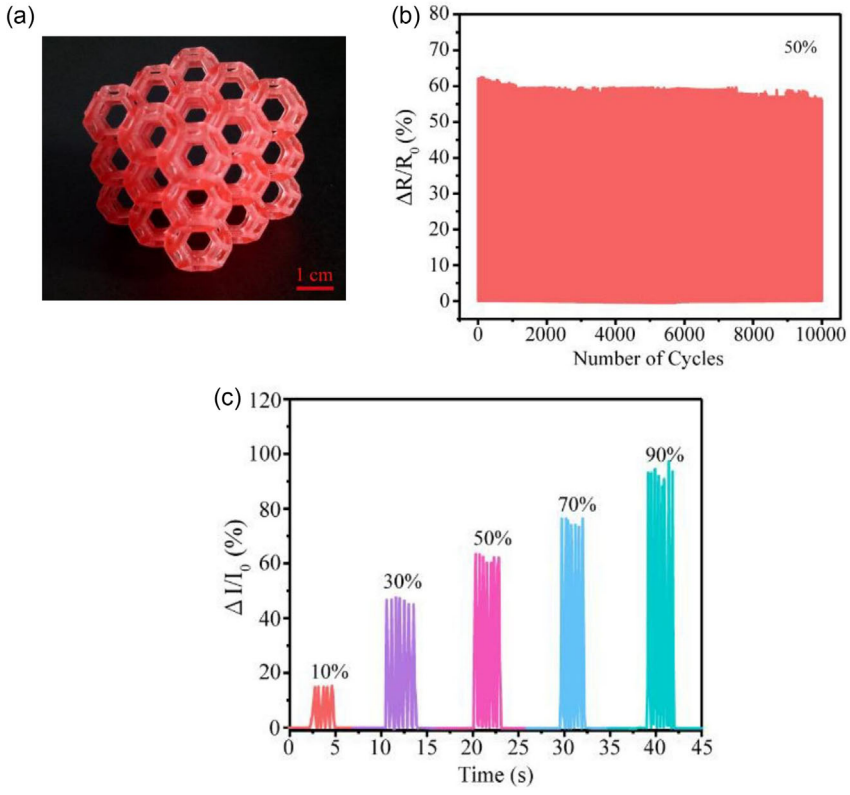

Figure 10. Self-healing sensor 3D-printed by SLA. a) Honeycomb was 3D-printed via SLA. b) The sensor produced a stable electrical signal and c) different currents according to the compression rate. Adapted with permission.[109] Copyright 2021, published by Elsevier B.V.

–NH_2, and –OH endowed the network with self-healing ability. Once the ink's feasibility was evaluated by printing different complex structures with a resolution of 10 μm, the authors shaped the material in a honeycomb 3D structure, possessing high flexibility and conductivity. The excellent compressive deformation (97%) and rebound were caused by the combination of hard (AAm/ChCl) and soft (MA/ChCl) domains of the material, but also by the honeycomb 3D shape, which is known to

cover the larger volume with less material, providing increased deformability. At a compression strain of 50%, the 3D-printed elastomer showed a stable electrical signal for 10 000 cycles. Moreover, the sensing unit was assessed to produce different currents under different compression rates, paving the way for its further development as a smart sensor. Finally, the sensor maintained its performance after multiple damage-healing cycles, due to its self-healing ability.

The authors developed a smart material for SLA 3D printing, demonstrating that complex geometries and material properties can endow soft sensors with advanced performance. In particular, self-healing behavior improved the durability of the sensor, holding potential for the fabrication of 3D sensors that can withstand damage, thus being suitable for long-term applications.

5. Discussion

This review described the potential advantages and drawbacks of 3D printing of soft materials and sensors, based on the AM different technologies. The DIW is the most common technique due to its versatility and the opportunity for multi-material printing. Nevertheless, VP-3D printing is emerging as a promising tool to produce complex structures with extraordinary resolution, while FFF represents a reliable solution because of its simplicity and cost-effectiveness.

However, a clear outcome of this review is that each 3D printing technology sets some requirements that the soft inks must fulfill. The different constraints can be summarized as follows. First, materials for DIW must possess a thixotropic behavior that can be achieved or improved by adding rheological adjusters. Inks for VP technologies must be photocurable and possess low viscosity. There are some commercial photocurable elastomers available, but they are limited in elongation as compared to silicone rubbers.[110] To overcome this issue, researchers focused on the synthesis of customizable, "home-made" photocurable elastomers and hydrogels.[104,107,110] Finally, materials for FFF are poorly customizable due to the difficulties in fabricating filaments.

In the first place, the aforementioned issues concern the soft matrixes, but once the fillers are added, the properties of the composite material must be re-evaluated to assess its suitability for the 3D printing technology.

The fillers lead to several issues, such as altered viscosity, opacity, and the occurrence of reinforcers' aggregation. These can impact both the material's processability and the final object's properties. Then, it is necessary to consider some aspects to optimize the printing of the composite ink and to fabricate a soft sensor with improved performance. Firstly, the process parameters (e.g., the pressure of the nozzle for DIW, the irradiation time for DLP) play a crucial role in achieving a self-standing object with high fidelity to the CAD model. Furthermore, the concentration and the morphology of the fillers are fundamental: the load and the size must ensure a proper trade-off between conductivity, processability, and mechanical properties.

The morphology of the fillers has a substantial impact on the final electrical properties of the sensors. 0D nanofillers (i.e., nanoparticles) interact poorly with the neighboring fillers, resulting in nonlinearity, limited sensitivity, and low cyclic durability.[111] On the contrary, the addition of 1D (nanowhiskers, nanofibers, nanotubes)[70,112,113] or 2D (nanosheets)[69] nanomaterials leads to sensing materials with improved performances due to their spatial alignments and exceptional electro-mechanical properties. In particular, the potential to produce interconnected conductive networks instead of dispersed individual fillers is crucial to improve the sensor's performance. In this regard, nanofillers with high aspect ratio are preferable as they can form conductive networks at low concentrations limiting the decremental impact on mechanical properties and processability of the composite materials. AM represents a scalable and reproducible tool to develop 3D nano-conductive networks, benefiting from the free digital computer-assisted design and the precise fabrication process.

Nevertheless, researchers have also proposed alternative solutions to the direct addition of nanofillers in the ink, such as dip and spray coating methods.[114] Applying a conductive coating is generally time-consuming because the procedure may be repeated several times. Moreover, some expedients are needed to obtain stable adhesion on the 3D sample, as in the reported case studies. Noteworthy, this approach limits the effects of the fillers on the mechanical, optical, and rheological properties of the soft material. Hence, this aspect enlarges the palette of printable materials that still maintain the required softness.

Despite the challenges, the literature demonstrates that it is possible to fabricate soft sensors via AM technologies using various materials, as listed in **Table 4**. Elastomers, hydrogels, polymers, and conductive fillers have been employed for various types of sensors and their parts. As for the dielectric or the flexible matrix, elastomers and soft polymers such as PDMS,[84,115] PET,[116] EcoFlex silicone,[117] and polyurethanes[47,118,119] are frequently employed. Instead, deformable transductors are made of conductive polymers (PDMS, PTFE, PU, rubbers, PVC) containing liquid conductors or conductive nanofillers (CNTs, graphene, metal nanowires).[22,83]

Even challenging, the 3D printing of soft sensors leads to impressive gains, as discussed in the previous sections.

The fabrication of the whole sensor and, potentially, of the entire robotic device in a seamless process represents a key ambition of the field. By exploiting multimaterial printing, AM holds a strong potential for this purpose, but, until now, the process is still characterized by a strong steps-processing nature. 3D printing is usually aimed at producing either one sensor component, which is then assembled into the others, or a mold through which the soft material can be shaped. As seen in the previous sections, printing a mold as a template for a soft sensor is useful to exploit materials, such as commercial silicones, that possess high deformability but are difficult to 3D print in complex shapes. Nevertheless, this approach is challenging to adapt for fabricating sensors with finer resolutions, and careful designs of the mold are required to produce complex parts such as lattices.

In contrast, the manual assembling of the sensor's elements allows the incorporation of materials unsuitable for 3D printing (e.g., copper electrodes). Still, the process is poorly reproducible and causes weak interlayer adhesion issues. Moreover, the wiring of the fabricated device remains an issue. Nevertheless, as reported in this review, examples of all-in-one fabrication of sensors exist. In some cases, the seamless fabrication not only saved time and materials, but it also improved the sensors' performance by providing a better adhesion between its

Table 4. Examples of sensors fabricated via 3D printing.

Material	Technology	Sensor	Element	Reference	Application
Graphene nanoplatelets (GNPs)/TPU	FFF	Resistive	Sensing unit	[70]	Pressure
PDMS	DIW	Capacitive	Dielectric layer	[86]	Pressure
Graphene/Silicone	FFF	Resistive	Sensing unit	[63]	Compression
Silicone	DIW	Resistive	Sensing unit	[123]	Pressure
Styrene–ethylene–butylene–styrene block copolymer	FFF	Resistive	Sensing unit	[69]	Compression/ stretching
CNT/TPU	DLP	Resistive	Sensing unit	[103]	Pressure
PDMS	DIW	Resistive	Substrate	[85]	Strain, Pressure
Carbon black/TPU	DIW	Resistive	Sensing unit	[85]	Strain, Pressure
Ag/TPU	DIW	Resistive	Electrode	[105]	Compression
Deep eutectic solvents (PDESs)	SLA	Resistive	Sensing unit	[105]	Compression
CNT/silicone	DIW	Resistive	Sensing unit	[84]	Tactile
Cu/Silicone	DIW	Resistive	Electrode	[84]	Tactile
CNT/PDMS	DIW	Resistive	Sensing unit	[51]	Compression
(PAAm/PEGDA/Mg^{2+}) hydrogel	DLP	Capacitive	Electrode	[47]	Pressure
Polyurethane acrylate	DLP	Capacitive	Dielectric	[47]	Pressure
Polydimethylacrylamide/ octadecyl acrylate hydrogel	DLP	Capacitive	Conductive layer	[124]	Pressure
PDMS/liquid metal	DIW	Resistive	Sensing unit	[125]	Tactile
PLA	FFF	Resistive	Mold	[62]	Strain
Silicone/CF	casting		Sensing unit	[62]	Strain
PLA	FFF	Resistive	Mold	[130]	Tactile
Graphene/PDMS	casting		Sensing unit	[130]	Tactile
PDMS	DIW	Capacitive	Dielectric	[86]	Pressure
Commercial TPU (Ninjaflex)	FFF	Resistive	Flexible Encapsulment	[120]	Strain
CNT/PLA			Sensing unit	[120]	Strain
Carbon black/TPU	FFF	Capacitive	Electrodes	[115]	Normal Force
TPU	FFF	Capacitive	Dielectric	[115]	Normal Force
PLA	FFF	Capacitive	Dielectric	[126]	Force
Carbon black/PLA	FFF	Capacitive	Electrode	[126]	Force

elements.[47,109] This confirms that 3D printing can be a step towards the straightforward fabrication of the robotic device, imparting enhanced properties.

The other aspect is related to the shape and the microstructure of the sensor. In this regard, AM enables the development of complex 3D structures with exceptional ease and scalability, in a more organic and customizable way, compared to traditional technologies.[120] Therefore, the investigation of AM's convenience in developing soft sensors passes by understanding the benefits of the 3D shape. In this regard, the impact of geometrical features on the material's deformability has been widely reported and discussed in this review. The creation of intricate, voids-provided structure enhances the inherent softness of the material, thus improving the sensor's performance (i.e., its sensitivity).

Moreover, the ability to increase and program mechanical deformations can be exploited to create materials with unconventional properties. For instance, the possibility to obtain a negative Poisson coefficient leads to the expansion in both length and width under stretching and shrinkage in both directions in response to compression. This enhances indentation resistance, shear resistance, and fracture toughness and improves the sensitivity by causing larger disconnections in the conducive networks.[62] Generally, this exceptional behavior can be employed in many electronic and sensing applications.[121,122] Furthermore, the 3D morphology achieved via AM can be used to obtain the so-called multi-directional sensing, i.e., the ability to discriminate different mechanical stimuli and/or to distinguish the stress' direction. Multidirectional sensing, which is already exhibited by many bio-receptors, is crucial to grant a safe interaction with the surroundings and to endow the robot with comprehension of its current state.[123] Although multidirectional sensing is still in its infancy, many efforts have been devoted to the understanding of the relationship between this ability and 2D/3D microstructures that exhibit distinct states of deformation and stress concentration according to the acting, mechanical input (shear, tensile, normal, bending).[124–126]

Due to these appealing opportunities, researchers investigated different strategies to fabricate soft mechanical sensors via 3D printing, with the main approaches summarized in **Table 5**. Advantages and drawbacks characterize each method, proving

Table 5. Summary of the main approaches for 3D printing of soft mechanical sensors. For each methodology, the advantages and drawbacks are summarized.

3D PRINTING APPROACHES FOR SOFT MECHANICAL SENSORS					
3D Architecture		Multi-material		Electrical conductivity	
Direct 3D Printing	Mold 3D Printing	Post assembling	Multi-material 3D Printing	Conductive inks	Dip Coating
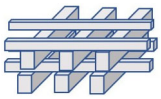	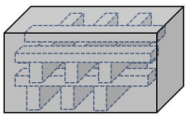	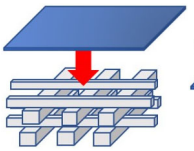		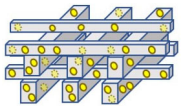	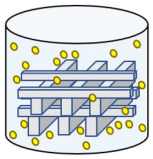
✓ Fast	✓ More materials available	✓ Simple	✓ Good reproducibility	✓ Conductive particles or polymers can be used	✓ Conductive particles or polymers can be used
× Material must be printable	✓ The mold can be dissolved (sacrificial molding)	✓ More materials available	✓ Strong interface and adhesion	✓ Build Conductivity	✓ Printability is not affected
	× Long fabrication time	× Weak interface	✓ Fast fabrication	✓ Fast fabrication	× Slow process
	× High complexity and fine features can not be obtained	× Low adhesion	× All the materials must be printable	× Nano-fillers modify the properties of the matrix	× Treatments are required to obtain a good interface
		× Poor reproducibility			× Only the surface is conductive

that the field is promising but still emerging, needing more investigation to pave the way for large-scale applications.

6. Conclusion

Nowadays, conventional subtractive techniques and molding represent the most common and economic tools for fabricating sensors. Nevertheless, these approaches are still limited by the low design freedom and slow and tedious production steps. 3D printing has emerged as a convenient alternative that addresses these obstacles, which is particularly beneficial in fabricating complex shapes. This article exposes the printing technologies and materials used for soft mechanical sensors by reporting case studies in which AM is successfully employed. Nevertheless, 3D printing in soft sensors is still challenging and allows for the investigation and development of innovative materials and processes. In view of the advancing demand for sensing technologies, the combination of AM, soft materials, and 3D geometries has the potential to implement innovative devices for future research and applications.

Acknowledgements

This work received funding from the European Union's Horizon 2020 research and innovation programme under grant agreement No. 863212 (PROBOSCIS project).

Conflict of Interest

The authors declare no conflict of interest.

Keywords

3D printing, capacitive sensors, resistive sensors, soft mechanical sensors, soft robots

Received: October 24, 2022
Revised: December 22, 2022
Published online: February 9, 2023

[1] M. Cianchetti, C. Laschi, A. Menciassi, P. Dario, *Nat. Rev. Mater.* **2018**, *3*, 143.
[2] C. Majidi, *Adv. Mater. Technol.* **2019**, *4*, 180477.
[3] M. Park, J. Park, U. Jeong, *Nano Today* **2014**, *9*, 244.
[4] C. Ahn, X. Liang, S. Cai, *Adv. Mater. Technol.* **2019**, *4*, 1900185.
[5] J. Shintake, V. Cacucciolo, D. Floreano, H. Shea, *Adv. Mater.* **2018**, *30*, 1707035.
[6] B. P. Mahale, D. Bodas, S. A. Gangal, in *NEMS 2011 - 6th IEEE Int. Conf. Nano/Micro Engineered and Molecular Systems*, IEEE, Piscataway, NJ **2011**, p. 658.
[7] Y. Jiang, J. Zhou, C. Feng, H. Shi, G. Zhao, Y. Bian, *J. Mater. Sci.* **2020**, *55*, 15709.
[8] E. Sachyani Keneth, A. Kamyshny, M. Totaro, L. Beccai, S. Magdassi, *Adv. Mater.* **2021**, *33*, 2003387.
[9] M. Izadifar, D. Chapman, P. Babyn, X. Chen, M. E. Kelly, *Tissue Eng. - Part C Methods* **2018**, *24*, 74.
[10] S. Kim, H. Seong, Y. Her, J. Chun, *Fash. Text.* **2019**, *6*, 9.
[11] T. H. Kim, J. Vanloo, W. S. Kim, *Adv. Mater. Technol.* **2021**, *6*, 2000938.
[12] T. D. Ngo, A. Kashani, G. Imbalzano, K. T. Q. Nguyen, D. Hui, *Composites, Part B* **2018**, *143*, 172.
[13] J. Walker, T. Zidek, E. Al, *Actuators* **2020**, *9*, 3.
[14] S. A. Wilson, L. M. Cross, C. W. Peak, A. K. Gaharwar, *ACS Appl. Mater. Interfaces* **2017**, *9*, 43449.
[15] S. Lee, Y. Kim, D. Park, J. Kim, *Compos. Commun.* **2021**, *26*, 100796.
[16] D. Jung, K. Kang, H. Jung, D. Seong, S. An, J. Yoon, W. Kim, M. Shin, H. W. Baac, S. Won, C. Shin, D. Son, *Micromachines* **2021**, *12*, 933.
[17] A. F. Carvalho, B. Kulyk, A. J. S. Fernandes, E. Fortunato, F. M. Costa, *Adv. Mater.* **2021**, *34*, 2101326.
[18] L. Y. Zhou, J. Fu, Y. He, *Adv. Funct. Mater.* **2020**, *30*, 2000187.
[19] C. Liu, N. Huang, F. Xu, J. Tong, Z. Chen, X. Gui, Y. Fu, C. Lao, *Polymers* **2018**, *10*, 629.
[20] Y. Lu, M. Chandra, Z. Guo, J. Jeon, E. K. Wujcik, *Biosens. Bioelectron.* **2019**, *123*, 167.
[21] M. Amjadi, K. U. Kyung, I. Park, M. Sitti, *Adv. Funct. Mater.* **2016**, *26*, 1678.

[22] F. Han, M. Li, H. Ye, G. Zhang, *Nanomaterials* **2021**, *11*, 1220.
[23] Z. Luo, X. Hu, X. Tian, C. Luo, H. Xu, Q. Li, Q. Li, J. Zhang, F. Qiao, X. Wu, V. E. Borisenko, J. Chu, *Sensors* **2019**, *19*, 1250.
[24] M. Amjadi, Y. J. Yoon, I. Park, *Nanotechnology* **2015**, *26*, 375501.
[25] R. A. Batista, C. G. Otoni, P. J. P. Espitia, *Fundamentals of Chitosan-Based Hydrogels: Elaboration and Characterization Techniques* (Eds: A.-M. Holban, A. M. Grumezescu), Elsevier Inc., Bucharest, RO **2019**.
[26] S. Choi, S. I. Han, D. Kim, D. Kim, T. Hyeon, D.-H. Kim, *Chem. Soc. Rev.* **2019**, *48*, 1566.
[27] I. A. Rashid, M. Shafiq, I. Yasir, Q. Gill, R. Nazar, F. Saeed, A. Afzal, H. Ehsan, A. Ali, *Polym. Bull.* **2020**, *77*, 1081.
[28] Y. Ding, J. Yang, C. R. Tolle, Z. Zhu, *Appl. Mater. Interfaces* **2018**, *10*, 16077.
[29] Y. Sun, Y. Chu, W. Wu, H. Xiao, *Carbohydr. Polym.* **2021**, *255*, 117489.
[30] H. R. Lim, H. S. Kim, R. Qazi, Y. T. Kwon, J. W. Jeong, W. H. Yeo, *Adv. Mater.* **2020**, *32*, 1901924.
[31] J. C. Costa, F. Spina, P. Lugoda, L. Garcia-Garcia, D. Roggen, N. Münzenrieder, *Technologies* **2019**, *7*, 35.
[32] J. Herzberger, J. M. Sirrine, C. B. Williams, T. E. Long, *Prog. Polym. Sci.* **2019**, *97*, 101144.
[33] S. C. Shit, P. Shah, *Natl. Acad. Sci. Lett.* **2013**, *36*, 355.
[34] I. Hong, S. Lee, *J. Ind. Eng. Chem.* **2013**, *19*, 42.
[35] F. Madsen, A. Daugaard, S. Hvilsted, A. Skov, *Macromol. Rapid Commun.* **2016**, *37*, 378.
[36] W. Triadji Nugroho, Y. Dong, A. Pramanik, J. Leng, *Composites, Part B* **2021**, *223*, 109104.
[37] S. Nozaki, T. Hirai, Y. Higaki, K. Yoshinaga, K. Kojio, A. Takahara, *Polymer* **2017**, *116*, 423.
[38] H. Li, J. T. Sun, C. Wang, S. Liu, D. Yuan, X. Zhou, J. Tan, L. Stubbs, C. He, *ACS Sustain. Chem. Eng.* **2017**, *5*, 7942.
[39] V. Kanyanta, A. Ivankovic, *J. Mech. Behav. Biomed. Mater.* **2010**, *3*, 51.
[40] P. Zhao, X. Hua, Y. Wang, J. Zhu, Q. Wen, *Mater. Sci. Eng., A* **2007**, *457*, 231.
[41] S. Manigandan, T. Praveenkumar, A. M. Al-Mohaimeed, K. Brindhadevi, A. Pugazhendhi, *Prog. Org. Coat.* **2021**, *150*, 105977.
[42] A. Abolins, R. Pomilovskis, E. Vanags, I. Mierina, S. Michalowski, A. Fridrihsone, M. Kirpluks, *Materials* **2021**, *14*, 894.
[43] S. Sair, S. Mansouri, O. Tanane, Y. Abboud, A. El Bouari, *SN Appl. Sci.* **2019**, *1*, 667.
[44] S. Ghosh, S. Ganguly, S. Remanan, S. Mondal, S. Jana, P. K. Maji, N. Singha, N. C. Das, *J. Mater. Sci. Mater. Electron.* **2018**, *29*, 10177.
[45] L. Zhang, D. Jiang, T. Dong, R. Das, D. Pan, C. Sun, Z. Wu, Q. Zhang, C. Liu, Z. Guo, *Chem. Rec.* **2020**, *20*, 948.
[46] P. Rahmani, A. Shojaei, *Adv. Colloid Interface Sci.* **2021**, *298*, 102553.
[47] X. Y. Yin, Y. Zhang, X. Cai, Q. Guo, J. Yang, Z. L. Wang, *Mater. Horiz.* **2019**, *6*, 767.
[48] M. Zhang, X. Tao, R. Yu, Y. He, X. Li, X. Chen, W. Huang, *J. Mater. Chem. A* **2021**, *10*, 12005.
[49] K. Tian, J. Bae, S. E. Bakarich, C. Yang, R. D. Gately, G. M. Spinks, M. in het Panhuis, Z. Suo, J. J. Vlassak, *Adv. Sci. News* **2017**, *29*, 1604827.
[50] A. Hamidi, Y. Tadesse, *Mater. Des.* **2020**, *187*, 108324.
[51] Q. Chen, J. Zhao, J. Ren, L. Rong, P. F. Cao, R. C. Advincula, *Adv. Funct. Mater.* **2019**, *29*, 1900469.
[52] S. Roh, D. P. Parekh, B. Bharti, S. D. Stoyanov, O. D. Velev, *Adv. Mater.* **2017**, *29*, 1701554.
[53] C. I. Idumah, C. M. Obele, *Surf. Interfaces* **2021**, *22*, 100879.
[54] M. Clingerman, J. A. King, K. H. Schulz, J. Meyers, *J. Appl. Polym. Sci.* **2002**, *83*, 1341.
[55] R. Taherian, *ECS J. Solid State Sci. Technol.* **2014**, *3*, 26.
[56] Z. M. Dang, K. Shehzad, J. W. Zha, T. Hussain, N. Jun, J. Bai, *Jpn. J. Appl. Phys.* **2011**, *50*, 080214.
[57] M. Khalifa, G. S. Ekbote, S. Anandhan, G. Wuzella, H. Lammer, A. R. Mahendran, *J. Appl. Polym. Sci.* **2020**, *137*, 49364.
[58] L. R. Viannie, N. R. Banapurmath, M. E. M. Soudagar, A. V. Nandi, N. Hossain, A. Shellikeri, V. Kaulgud, M. A. Mujtaba, S. A. Khan, M. Asif, *J. Environ. Chem. Eng.* **2021**, *9*, 106550.
[59] J. Lewis, J. E. Smay, J. Stuecker, J. Cesarana, *J. Am. Ceram. Soc.* **2006**, *3609*, 3599.
[60] I. Karakurt, L. Lin, *Curr. Opin. Chem. Eng.* **2020**, *28*, 134.
[61] C. Liu, H. Qin, P. T. Mather, *J. Mater. Chem.* **2007**, *17*, 1543.
[62] B. Taherkhani, M. B. Azizkhani, J. Kadkhodapour, A. P. Anaraki, S. Rastgordani, *Sens. Actuators, A* **2020**, *305*, 111939.
[63] E. Davoodi, H. Montazerian, R. Haghniaz, A. Rashidi, S. Ahadian, A. Sheikhi, J. Chen, A. Khademhosseini, A. S. Milani, M. Hoorfar, E. Toyserkani, *ACS Nano* **2020**, *14*, 1520.
[64] J. Z. Gul, M. Sajid, M. M. Rehman, G. Uddin, I. Shah, K. Kim, J. Lee, K. H. Choi, *Sci. Technol. Adv. Mater.* **2018**, *19*, 244.
[65] R. B. Kristiawan, F. Imaduddin, D. Ariawan, . Ubaidillah, Z. Arifin, *Open Eng.* **2021**, *11*, 639.
[66] E. L. Gilmer, D. Miller, C. A. Chatham, C. Zawaski, J. J. Fallon, A. Pekkanen, T. E. Long, C. B. Williams, M. J. Bortner, *Polymer* **2018**, *152*, 51.
[67] K. Bryll, E. Piesowicz, P. Szymański, W. Slaczka, M. Pijanowski, *MATEC Web Conf.* **2018**, *237*, 02006.
[68] S. Wickramasinghe, T. Do, P. Tran, *Polymers* **2020**, *12*, 1529.
[69] Z. Li, B. Li, B. Chen, J. Zhang, Y. Li, *Nanotechnology* **2021**, *32*, 395503.
[70] R. Yu, T. Xia, B. Wu, J. Yuan, L. Ma, G. J. Cheng, F. Liu, *ACS Appl. Mater. Interfaces* **2020**, *12*, 35291.
[71] M. Gastaldi, F. Cardano, M. Zanetti, G. Viscardi, C. Barolo, S. Bordiga, S. Magdassi, A. Fin, I. Roppolo, *ACS Mater. Lett.* **2021**, *3*, 1.
[72] J. Suriboot, A. C. Marmo, B. K. D. Ngo, A. Nigam, D. Ortiz-Acosta, B. L. Taic, M. A. Grunlan, *Soft Matter* **2021**, *17*, 4133.
[73] M. M. Durban, J. M. Lenhardt, A. S. Wu, W. Small, T. M. Bryson, L. Perez-Perez, D. T. Nguyen, S. Gammon, J. E. Smay, E. B. Duoss, J. P. Lewicki, T. S. Wilson, *Macromol. Rapid Commun.* **2018**, *39*, 1700563.
[74] B. Ye, C. Song, H. Huang, Q. Li, C. An, *Def. Technol.* **2020**, *16*, 588.
[75] J. Vadillo, I. Larraza, T. Calvo-correas, N. Gabilondo, C. Derail, A. Eceiza, *Materials* **2021**, *14*, 3287.
[76] Z. Jiang, B. Diggle, M. L. Tan, J. Viktorova, C. W. Bennett, L. A. Connal, *Adv. Sci.* **2020**, *7*, 2001379.
[77] A. Shahzad, I. Lazoglu, *Composites, Part B* **2021**, *225*, 109249.
[78] K. T. Chen, D. C. Cheng, J. T. Lin, H. W. Liu, *Polymers* **2019**, *11*, 1640.
[79] Y. Guo, Y. Liu, J. Liu, J. Zhao, H. Zhang, Z. Zhang, *Composites, Part A* **2020**, *135*, 105903.
[80] J. W. Kopatz, J. Unangst, A. W. Cook, L. N. Appelhans, *Addit. Manuf.* **2021**, *46*, 102159.
[81] P. J. Scott, D. A. Rau, J. Wen, M. Nguyen, C. R. Kasprzak, C. B. Williams, T. E. Long, *Addit. Manuf.* **2020**, *35*, 101393.
[82] C. Xu, B. Quinn, L. L. Lebel, D. Therriault, G. L'espérance, *ACS Appl. Mater. Interfaces* **2019**, *11*, 8499.
[83] Z. Wang, X. Guan, H. Huang, H. Wang, W. Lin, Z. Peng, *Adv. Funct. Mater.* **2019**, *29*, 1807569.
[84] W. Yang, Y. Liu, W. Xu, H. Y. Nie, *IEEE Sens. J.* **2021**, *21*, 10473.
[85] Z. Tang, S. Jia, C. Zhou, B. Li, *ACS Appl. Mater. Interfaces* **2020**, *12*, 28669.
[86] A. Bagheri, J. Jin, *ACS Appl. Polym. Mater.* **2019**, *1*, 593.
[87] S. S. Labana, *J. Macromol. Sci.* **1974**, *11*, 299.
[88] M. Kaur, A. K. Srivastava, *J. Macromol. Sci. - Polym. Rev.* **2002**, *42*, 481.
[89] B. C. Gross, J. L. Erkal, S. Y. Lockwood, C. Chen, D. M. Spence, *Anal. Chem.* **2014**, *86*, 3240.
[90] X. Xu, C. Guan, L. Xu, Y. H. Tan, D. Zhang, Y. Wang, H. Zhang, D. J. Blackwood, J. Wang, M. Li, J. Ding, *ACS Nano* **2020**, *14*, 937.
[91] Z. Zhao, X. Tian, X. Song, *J. Mater. Chem. C* **2020**, *8*, 13896.

[92] G. Gonzalez, A. Chiappone, I. Roppolo, E. Fantino, V. Bertana, F. Perrucci, L. Scaltrito, F. Pirri, M. Sangermano, *Polymer* **2017**, *109*, 246.
[93] W. Lim, J. Bae, M. Seo, J. Min, J. Lee, S. Hyun, Y. Jung, P. Huh, *Addit. Manuf.* **2022**, *51*, 102625.
[94] X. Li, R. Yu, Y. He, Y. Zhang, X. Yang, X. Zhao, W. Huang, *ACS Macro Lett.* **2019**, *8*, 1511.
[95] G. Gonzalez, A. Chiappone, K. Dietliker, C. F. Pirri, I. Roppolo, *Adv. Mater. Technol.* **2020**, *5*, 2000374.
[96] N. Bhattacharjee, C. Parra-Cabrera, Y. T. Kim, A. P. Kuo, A. Folch, *Adv. Mater.* **2018**, *30*, 1800001.
[97] Y. Hu, G. Zhu, J. Zhang, J. Huang, X. Yu, Q. Shang, R. An, C. Liu, L. Hu, Y. Zhou, *Molecules* **2021**, *26*, 5455.
[98] H. Chen, S.-Y. Lee, Y.-M. Lin, *Polymers* **2020**, *12*, 1500.
[99] P. Marx, A. Romano, I. Roppolo, A. Chemelli, I. Mühlbacher, W. Kern, S. Chaudhary, T. Andritsch, M. Sangermano, F. Wiesbrock, *Macromol. Mater. Eng.* **2019**, *304*, 1900515.
[100] T. Zhao, R. Yu, S. Li, X. Li, Y. Zhang, X. Yang, X. Zhao, C. Wang, Z. Liu, R. Dou, W. Huang, *Appl. Mater. Interfaces* **2019**, *11*, 14391.
[101] H. Xiang, X. Wang, Z. Ou, G. Lin, J. Yin, Z. Liu, *Prog. Org. Coat.* **2019**, *137*, 105372.
[102] T. J. Wallin, J. H. Pikul, S. Bodkhe, B. N. Peele, B. C. Mac Murray, D. Therriault, B. W. McEnerney, R. P. Dillon, E. P. Giannelis, R. F. Shepherd, *J. Mater. Chem. B* **2017**, *5*, 6249.
[103] S. Lantean, G. Barrera, C. F. Pirri, P. Tiberto, M. Sangermano, I. Roppolo, G. Rizza, *Adv. Mater. Technol.* **2019**, *4*, 1900505.
[104] X. Y. Yin, Y. Zhang, J. Xiao, C. Moorlag, J. Yang, *Adv. Funct. Mater.* **2019**, *29*, 1904716.
[105] Q. Mu, L. Wang, C. K. Dunn, X. Kuang, F. Duan, Z. Zhang, H. J. Qi, T. Wang, *Addit. Manuf.* **2017**, *18*, 74.
[106] Y. M. Yin, H. Y. Li, J. Xu, C. Zhang, F. Liang, X. Li, Y. Jiang, J. W. Cao, H. F. Feng, J. N. Mao, L. Qin, Y. F. Kang, G. Zhu, *ACS Appl. Mater. Interfaces* **2021**, *13*, 10388.
[107] S. Peng, Y. Li, L. Wu, J. Zhong, Z. Weng, L. Zheng, Z. Yang, J. T. Miao, *ACS Appl. Mater. Interfaces* **2020**, *12*, 6479.
[108] C.-C. Kim, H.-H. Lee, K. H. Oh, J.-H. Sun, *Science* **2016**, *353*, 6300.
[109] L. Cai, G. Chen, B. Su, M. He, *Chem. Eng. J.* **2021**, *426*, 130545.
[110] D. K. Patel, A. H. Sakhaei, M. Layani, B. Zhang, Q. Ge, S. Magdassi, *Adv. Mater.* **2017**, *29*, 1606000.
[111] Y. Lee, J. Kim, H. Joo, M. S. Raj, R. Ghaffari, D. H. Kim, *Adv. Mater. Technol.* **2017**, *2*, 1700053.
[112] S. Gong, W. Schwalb, Y. Wang, Y. Chen, Y. Tang, J. Si, B. Shirinzadeh, W. Cheng, *Nat. Commun.* **2014**, *5*, 3132.
[113] M. O. Tas, M. A. Baker, M. G. Masteghin, J. Bentz, K. Boxshall, V. Stolojan, *Appl. Mater. Interfaces* **2019**, *11*, 39560.
[114] M. Seo, S. Hwang, T. Hwang, J. Yeo, *Materials***2019**, *12*, 2955.
[115] X. Yu, Y. Li, H. Yu, *Electron. Lett.* **2019**, *55*, 999.
[116] S. Li, R. Li, T. Chen, X. Xiao, *IEEE Sens. J.* **2020**, *20*, 14436.
[117] M. Ntagios, S. Dervin, R. Dahiya, in *IEE FLEPS Conf.*, IEEE, Piscataway, NJ **2021**, pp. 1–4.
[118] J. Nichols Cook, A. Sabarwal, H. Clewer, W. Navaraj, in *2020 IEEE SENSORS*, IEEE, Piscataway, NJ **2020**, pp. 11–14.
[119] L. Y. W. Loh, U. Gupta, Y. Wang, C. C. Foo, J. Zhu, W. F. Lu, *Adv. Eng. Mater.* **2021**, *23*, 2001082.
[120] B. Zhuo, S. Chen, M. Zhao, X. Guo, *IEEE J. Electron Devices Soc.* **2017**, *5*, 219.
[121] F. La Malfa, S. Puce, F. Rizzi, M. De Vittorio, *Nanomaterials* **2020**, *10*, 2365.
[122] J. Ko, S. Bhullar, Y. Cho, P. C. Lee, M. Byung-Guk Jun, *Smart Mater. Struct.* **2015**, *24*, 075027.
[123] J. Lee, S. Pyo, M. Kim, *Nanotechnology* **2018**, *29*, 055501.
[124] S. Mousavi, D. Howard, F. Zhang, J. Leng, C. H. Wang, *ACS Appl. Mater. Interfaces* **2020**, *12*, 15631.
[125] N. A. A. Ridzuan, N. Miki, *Micromachines* **2018**, *10*, 18.
[126] X. Chen, X. Zhang, D. Xiang, Y. Wu, C. Zhao, H. Li, Z. Li, P. Wang, Y. Li, *Mater. Lett.* **2022**, *306*, 130935.
[127] L. Gan, S. Shang, S. X. Jiang, *Composites, Part B* **2016**, *84*, 294.
[128] X. Liu, C. Li, Z. Wang, Y. Li, J. Huang, H. Yu, *IEEE Sens. J.* **2021**, *21*, 9798.
[129] C. Tugui, G. T. Stiubianu, M. S. Serbulea, M. Cazacu, *Polym. Chem.* **2020**, *11*, 3271.
[130] Y. Liu, Y. Xu, R. Avila, C. Liu, Z. Xie, L. Wang, X. Yu, *Nanotechnology* **2019**, *30*, 414001.
[131] R. Chen, X. Xu, Y. Danfeng, X. Chuanghong, M. Liu, J. Huang, T. Mao, C. Zheng, Z. Wang, W. Xu, *J. Mater. Chem. C* **2018**, *6*, 1193.
[132] H. Zhou, L. Zheng, Q. Meng, R. Tang, Z. Wang, B. Dang, X. Shen, Q. Sun, *J. Mater. Chem.* **2021**, *9*, 12895.
[133] F. Ye, M. Li, D. Ke, L. Wang, Y. Lu, *Adv. Mater. Technol.* **2019**, *4*, 1900346.
[134] S. Xia, S. Song, F. Jia, G. Gao, *J. Mater. Chem. B* **2019**, *7*, 4638.
[135] S. Pan, M. Xia, H. Li, X. Jiang, P. He, Z. Sun, Y. Zhang, *J. Mater. Chem. C* **2020**, *8*, 2827.
[136] M. Zhang, G. Chen, M. Lei, J. Lei, D. Li, H. Zheng, *Int. J. Biol. Macromol.* **2021**, *182*, 385.
[137] S. Jang, A. Boddorff, D. J. Jang, J. Lloyd, K. Wagner, N. Thadhani, B. Brettmann, *Addit. Manuf.* **2021**, *47*, 102313.
[138] S. Xiang, S. Chen, M. Yao, F. Zheng, Q. Lu, *J. Mater. Chem. C* **2019**, *7*, 9625.
[139] T. Li, K. Nakajima, M. Calisti, C. Laschi, R. Pfeifer, in *2012 IEEE Int. Conf. Mechatronics Automation ICMA*, IEEE, Piscataway, NJ **2012**, p. 948.

Diana Cafiso received her M.Sc. degree in material engineering in 2020 from Politecnico di Torino, Italy. She is currently pursuing her Ph.D. at the Soft Biorobotic Perception (SBRP) lab of the Istituto Italiano di Tecnologia (IIT) and at the Politecnico di Torino, Italy. Her research interests are the development of materials for soft sensing and actuation, composite polymers, 3D printing, and photopolymerization.

Simone Lantean received his M.Sc. degree in materials engineering from Politecnico di Torino, Italy, in 2017. In 2021, he earned his Ph.D. in materials science and technology from Politecnico di Torino, Italy, and Ecòle Polytechnique, France, in a co-tutored project on the 3D printing of magnetic nanocomposites with programmable microstructures. In 2021, he joined the Soft BioRobotics Perception (SBRP) lab at Istituto Italiano di Tecnologia (IIT), Italy, as a postdoctoral researcher focusing on soft sensors and artificial skins.

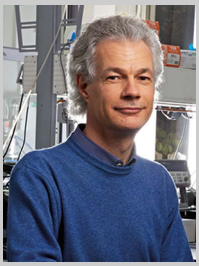

Candido Fabrizio Pirri Director of the Center for Sustainable Future Technologies of the Istituto Italiano di Tecnologia. Full professor of Physics of Matter at Politecnico di Torino. From 2011 to 2016, he was director of the Center for Space Human Robotics of the Italian Institute of Technology. Scientific interests: Micro and nanodevices for energy and environment, micro and nanotechnologies for smart manufacturing, graphene and 2D materials for energy, bioenergy, and environment (solar cells, supercapacitors, microbial fuel cells), nanomaterials and nanostructures for CO_2 trapping and reduction, nanostructures for H_2 trapping, H_2 storage and use, multifunctional materials for 3D printing.

Lucia Beccai is a tenured senior researcher at the Istituto Italiano di Tecnologia (IIT), Italy, leader of the Soft BioRobotic Perception (SBRP) lab. She was assistant professor in biomedical engineering at the Biorobotics Institute of Scuola Superiore Sant'Anna, Italy, until 2009 and has a Ph.D. in microsystem engineering. Her research belongs to both biorobotics and soft robotics with the final aim of achieving soft sensing and perceptive soft robotic solutions for intelligent and safe interaction. Specific topics include bioinspired multimodal tactile systems, soft robotic systems for active and passive touch, milli- and micro-scale fabrication technologies for 3D active structures, soft versatile grasping and manipulation.